Invariance Learning based on Label Hierarchy

Anonymous Author(s)
Affiliation
Address
email

Abstract

Deep Neural Networks inherit biased correlations embedded in training data and hence may fail to predict desired labels on unseen domains (or environments), which have different distributions from the domain to provide training data. Invariance Learning (IL) has been developed recently to overcome this shortcoming; using training data in many domains, IL estimates such a predictor that is invariant to a change of domain. However, the requirement of training data in multiple domains is a strong restriction of using IL, since it demands expensive annotation. We propose a novel IL framework to overcome this problem. Assuming the availability of data from multiple domains for a classification task at a *higher* level, for which the labeling cost is lower, we estimate an invariant predictor for the target classification task with training data gathered in a *single* domain. Additionally, we propose two cross-validation methods for selecting hyperparameters of invariance regularization, which has not been addressed properly in existing IL methods. The effectiveness of the proposed framework, including the cross-validation, is demonstrated empirically. Theoretical analysis reveals that our framework can estimate the desirable invariant predictor with a hyperparameter fixed correctly, and that such a preferable hyperparameter is chosen by the proposed CV methods under some conditions.

1 Introduction

Training data used in machine learning may contain features that are spuriously correlated to the labels of data. Deep Neural Networks (DNNs) often learn such biased correlations embedded in training data and hence may fail to predict desired labels of test data generated by a different distribution from one to provide training data. In classification of animal images, DNNs tend to misclassify cows on sandy beaches, since most training pictures are taken in green pastures and DNNs inherit context information in training [3, 9]. Another example is learning from medical data. Systems trained with data collected in one hospital do not generalize well to other hospitals; DNNs unintentionally extract environmental factors specific to a particular hospital in training [16–18].

Invariance Learning (IL) is a rapidly developed approach to overcome the issue of biased correlation, which is caused by some bias in the distribution of a training dataset [10–15, 21, 33–36, 54]. In this paper, we use the term *domain* to specify the bias in the distribution of a dataset. IL is thus a method for removing the influence of domain shits. Using training data from *multiple* domains, IL estimates a predictor *invariant* to the change of domains, aiming at keeping good performance in unseen domains as well as in the training domains.

While the IL approach has attracted much attention, requiring training data from multiple domains may hinder wide applications in practice; preparing training data in many domains often involves expensive data annotation. In real-world data, labels may be missing [42–45, 56–58] or incomplete [46–48]. Such data with incomplete annotation are not directly applicable to the standard IL meth-

Submitted to 36th Conference on Neural Information Processing Systems (NeurIPS 2022). Do not distribute.

ods; they must be re-annotated accurately, often at great financial or human expense. The high cost drives a strong need to establish a new IL framework without or with lower annotation costs.

To mitigate the problem of annotation cost, we propose a novel IL framework for the situation where the training data of target classification is given in only *one* domain, while the task of higher *label hierarchy*, which needs lower annotation cost, has data from multiple domains. Here, the task of higher *label hierarchy* means a classification task with coarser labels than those of the target classification. Figure 1 shows an example of label hierarchy. Consider the case where a target classification has 300 labels $\{\text{bird}_1, ..\text{bird}_{100}, \text{snake}_1, ..., \text{snake}_{100}, \text{turtle}_1, ..., \text{turtle}_{100}\}$ corresponding to 300 species. Then, the binary labels $\{\text{bird}, \text{reptile}\}$ are an example of labels in the higher hierarchy. The decrease in the number of classes reduces annotation time per image. Moreover, annotation of the binary labels does not require any expert knowledge, while annotation of the original 300 labels would requires expert knowledge about birds, snakes, and turtles. Hence, the new IL framework significantly reduces the annotation cost in comparison with previous IL methods; we need exhausting annotation of 300 classes only for one domain and just binary labels for other domains.

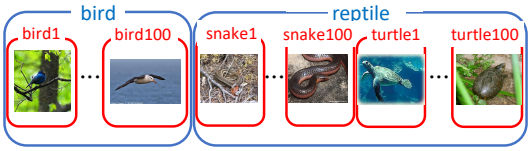

Figure 1: Example of Label hierarchy. Blue labels are in higher level of label hierarchy than red labels.

Another important issue in IL is hyperparameter selection. Most IL methods involve some hyperparameters to balance the classification accuracy and the degree of invariance. As [21] and [19] point out, in the literature of IL, the best performances of invariance had often been achieved by selecting the hyperparameters using test data from unseen domains. Moreover, [19] numerically demonstrated that, without using test data, simple methods of hyperparameter selection fail to find a preferable hyperparameter. It demonstrates a strong need for establishing an appropriate method of hyperparameter selection for IL.

We propose two methods of cross-validation (CV) for hyperparameter selection in our new IL framework. Since we assume training data of a single domain for the target task, it is impossible to estimate the deviation of the risks over the domains. Our CV methods mitigate the difficulty by using additional data from multiple domains in the higher label hierarchy. Theoretical analysis proves that our methods select a hyperparameter correctly under some conditions.

The main contributions of this paper are as follows:

- We establish a novel framework of invariance learning, which estimates an invariant predictor from a single domain data, assuming additional data from multiple domains for a classification task at a higher level.
- Under the framework, we propose two methods of cross-validation for selecting hyperparameters without accessing any samples from unseen target domains.
- Experimental studies verify that the proposed framework extracts an invariant predictor more effectively than other existing methods.
- We mathematically prove that our framework can estimate a correct invariant predictor with a hyperparameter fixed correctly and that such a preferable hyperparameter is selected by the proposed CV methods under some settings.

2 Invariance Learning based on Label Hierarchy

Notations Throughout this paper, the space of input features and finite class labels are denoted by $\mathcal{X}$ and $\mathcal{Y}$, respectively. For given predictor $f : \mathcal{X} \to \mathcal{Y}$ and random variable (X, Y) on $\mathcal{X} \times \mathcal{Y}$ with its probability $P_{X,Y}$, $\mathcal{R}^{(X,Y)}(f)$ denotes the risk of f on (X, Y); *i.e.*, $\mathcal{R}^{(X,Y)}(f) := \int l(f(x), y) dP_{X,Y}$, where $l : \mathcal{Y} \times \mathcal{Y} \to \mathbb{R}$ is a loss function. For $m \in \mathbb{N}_{>0}$, $[m]$ denotes the set $\{1, ..., m\}$. For a finite set A, $|A| \in \mathbb{N}$ denotes the number of elements in A.

2.1 Review of Invariance Learning

Following [10], to formulate the out-of-distribution (o.o.d.) generalization, we assume that the joint distribution of data (X^e, Y^e) depends on the domain (or environment) $e \in \mathcal{E}$, and consider the

dependence of a predictor f on the domain variable e. Suppose we are given training datasets $\mathcal{D}^e := \{(x_i^e, y_i^e)\}_{i=1}^{n^e} \sim P_{X^e,Y^e}$ i.i.d. from multiple domains $\mathcal{E}_{tr} \subset \mathcal{E}$. The final goal of the o.o.d. problem is to predict a desired label $Y^e \in \mathcal{Y}$ from $X^e \in \mathcal{X}$ for larger target domains $\mathcal{E} \supset \mathcal{E}_{tr}$. To discuss the o.o.d. performance, [10] introduced the o.o.d. risk

$$\mathcal{R}^{o.o.d.}(f) := \max_{e \in \mathcal{E}} \mathcal{R}^e(f), \tag{1}$$

where $\mathcal{R}^e(f) := \mathcal{R}^{(X^e,Y^e)}(f)$. This is the worst case risk over $\mathcal{E}$, including unseen domains $\mathcal{E} \setminus \mathcal{E}_{tr}$.

To solve (1), [10] estimates a predictor f that performs well in unseen domains $\mathcal{E} \setminus \mathcal{E}_{tr}$ as well as training domains $\mathcal{E}_{tr}$, namely a predictor *invariant* to a change of domains. The invariant predictor f is composed of two maps Φ and w; that is, $f = w \circ \Phi$ holds. A feature map $\Phi : \mathcal{X} \to \mathcal{H}$, which is often called an *invariance*, realizes a feature of $x \in \mathcal{X}$ in the feature space $\mathcal{H}$ with biased correlations in x removed. A predictor $w : \mathcal{H} \to \mathcal{Y}$ estimates the label of feature $\Phi(x)$. The estimation of an invariant predictor is implemented by solving the following optimization problem:

$$\min_{\Phi \in \mathcal{I}_{tr}, w:\mathcal{H}\to\mathcal{Y}} \sum_{e \in \mathcal{E}_{tr}} \mathcal{R}^e(w \circ \Phi), \tag{2}$$

where $\mathcal{I}_{tr}$ is the set of invariances captured by $\bigcup_{e \in \mathcal{E}_{tr}} \mathcal{D}^e$:

$$\mathcal{I}_{tr} := \left\{\Phi : \mathcal{X} \to \mathcal{H} \mid P(Y^{e_1}|\Phi(X^{e_1})) = P(Y^{e_2}|\Phi(X^{e_2})) \text{ for any } e_1, e_2 \in \mathcal{E}_{tr}\right\}.$$

This invariance is based on conditional independence as [14, 15, 40], while [10, 11] use a different type invariance based on $\operatorname{argmin}_w \mathcal{R}^e(w \circ \Phi)$ instead of $P(Y^e|\Phi(X^e))$. All IL methods estimate the invariance using the difference among $\mathcal{E}_{tr}$, assuming the availability of *multiple* training domains.

2.2 Invariance estimation by higher label data

Our goal is to make an invariant predictor from a single training domain $\mathcal{E}_{tr} = \{e^*\}$. In this case, (2) is reduced to the empirical risk minimization $\min_f \mathcal{R}^{e^*}(f)$ on e^*, and therefore the standard IL framework is not able to extract an invariance.

In this paper, we introduce an assumption that additional data $\mathcal{D}_{ad}^e$ for an another task (X^e, Z^e), which is in the higher label hierarchy than (X^e, Y^e), is available with respect to multiple domains $\mathcal{E}_{ad} \subset \mathcal{E}$. The task of higher hierarchy (X^e, Z^e) has a *coarser* label $Z^e \in \mathcal{Z}$ than $Y^e \in \mathcal{Y}$; more formally, Z^e is represented as $Z^e = g(Y^e)$ with a surjective label mapping $g : \mathcal{Y} \to \mathcal{Z}$ from the lower to the higher level in the label hierarchy. The example in Section 1 is formalized by a surjevtive function g as, setting $\mathcal{Y} := \{\text{bird}_1, .., \text{bird}_{100}, \text{turtle}_1, .., \text{turtle}_{100}, \text{snake}_1, .., \text{snake}_{100}\}$ and $\mathcal{Z} := \{\text{bird}, \text{reptile}\}$, $g(y) := \text{bird}$ if $y = \text{bird}_i$ ($i \in \{1, 2, ..., 100\}$) and $g(y) := \text{reptile}$ else.

By making use of $\{\mathcal{D}_{ad}^e\}_{e \in \mathcal{E}_{ad}}$, our objective for the invariant prediction is given by

$$\min_{\Phi \in \mathcal{I}_{ad}, w:\mathcal{H}\to\mathcal{Y}} \mathcal{R}^{e^*}(w \circ \Phi), \tag{3}$$

where $\mathcal{I}_{ad}$ is the set of invariances:

$$\mathcal{I}_{ad} := \left\{\Phi : \mathcal{X} \to \mathcal{H} \mid P(g(Y^{e_1})|\Phi(X^{e_1})) = P(g(Y^{e_2})|\Phi(X^{e_2})) \text{ for any } e_1, e_2 \in \mathcal{E}_{ad}\right\}.$$

Note that (3) evaluates the risk with a single training domain while the invariances are given by additional data of multiple domains.

2.3 Construction of objective function

Among several candidates of the loss and model design, we focus a probabilistic output case and evaluate its error by the cross entropy loss; that is, we model w by $p_\theta : \mathcal{H} \to \mathcal{P}_\mathcal{Y}$, where $\mathcal{P}_\mathcal{Y}$ denotes the set of probabilities on $\mathcal{Y}$ and θ denotes a model parameter. The risk is then written by

$$\mathcal{R}^e(p_\theta \circ \Phi) = \int -\log p_\theta(Y^e|\Phi(X^e)) dP_{X^e,Y^e}.$$

We aim to solve (3) by minimizing the following objective function:

$$\begin{aligned}\text{Objective}(\theta, \Phi) &:= \hat{\mathcal{R}}^{e^*}(p_\theta \circ \Phi) \\ &\quad + \lambda \cdot (\text{Dependence measure of } P(g(Y^e)|\Phi(X^e)) \text{ on } e \in \mathcal{E}_{ad}).\end{aligned} \tag{4}$$

Here, $\hat{\mathcal{R}}^{e^*}(p_\theta \circ \Phi)$ denotes the empirical risk of $p_\theta \circ \Phi$ on the training domain $\mathcal{E}_{tr} = \{e^*\}$ evaluated by $\mathcal{D}^{e^*}$: $\hat{\mathcal{R}}^{e^*}(p_\theta \circ \Phi) := -\frac{1}{|\mathcal{D}^{e^*}|}\sum_{(x^{e^*},y^{e^*})\in\mathcal{D}^{e^*}} \log p_\theta(y^{e^*}|\Phi(x^{e^*}))$. While we can consider some variations of invariance regularization, we adopt the one used in [10] and construct an objective function as

$$\text{Objective}(\theta, \theta_{ad}, \Phi) := \hat{\mathcal{R}}^{e^*}(p_\theta \circ \Phi) + \lambda \cdot \sum_{e\in\mathcal{E}_{ad}} \|\nabla_{\hat{\theta}_{ad}=\theta_{ad}} \hat{\mathcal{R}}^{(X^e,Z^e)}(p^{\mathcal{Z}|\mathcal{H}}_{\hat{\theta}_{ad}} \circ \Phi)\|^2. \tag{5}$$

Here, $p^{\mathcal{Z}|\mathcal{H}}_\theta : \mathcal{H} \to \mathcal{P}_\mathcal{Z}$ is the linear logistic regression model same as [10], Φ is a nonlinear neural network, and $\hat{\mathcal{R}}^{(X^e,Z^e)}(p^{\mathcal{Z}|\mathcal{H}}_{\theta_{ad}} \circ \Phi) := -\frac{1}{|\mathcal{D}^e_{ad}|}\sum_{(x^e,z^e)\in\mathcal{D}^e_{ad}} \log p^{\mathcal{Z}|\mathcal{H}}_{\theta_{ad}}(z^e|\Phi(x^e))$.

It is not obvious if the regularization term in (5) is valid as a dependence measure of $P(g(Y^e)|\Phi(X^e))$, since it was proposed for another type of invariance based on $\operatorname{argmin}_w \mathcal{R}^e(w \circ \Phi)$. The next lemma shows that these notions of invariance are the same in the current setting.

Lemma 1. *When modeling w by conditional probabilities, the following statements are equivalent:*

$$P(Z^e|\Phi(X^e)) \text{ does not depend on } e \Leftrightarrow \operatorname{argmin}_{p^{\mathcal{Z}|\mathcal{H}}_{\theta_{ad}}} \mathcal{R}^{(X^e,Z^e)}(p^{\mathcal{Z}|\mathcal{H}}_{\theta_{ad}} \circ \Phi) \text{ does not depend on } e,$$

where model $p^{\mathcal{Z}|\mathcal{H}}_{\theta_{ad}}$ in the right hand side runs over all probability densities.

While our objective function (5) is similar to the ones in [10, 21] in that they are composed of an empirical risk and an invariance regularization, the correctness has not been fully discussed so far. In Section 4, we will mathematically prove the correctness of (5) under some settings.

3 Hyperparameter selection method

3.1 Hyperparameter Selection in Invarance Learning

The objective function (5) has a hyperparameter λ to select, as is often the case with IL methods. The hyperparameter selection in IL has special difficulty, however; because the o.o.d. problem needs to predict Y^e on unseen domains, λ must be chosen without accessing any data in such unseen domains. It was reported in [19, 21] that the success of IL methods depends strongly on the careful choice of hyperparameters, and some of the results even used data from unseen domains in the choice. [19] reported also experimental results of various IL methods with two CV methods, training-domain validation (Tr-CV) and leave-one-domain-out validation (LOD-CV), and showed that the CV methods failed to select preferable hyperparameters. In the Colored MNIST experiment, for example, the accuracy of Invariant Risk Minimization [10] is 52.0% at best, which is about a random guess level.

The failure of the CV methods is caused by the improper design of the objective function for CV; they do not simulate the o.o.d. risk, which is the maximum risk over the domains. Tr-CV splits data in each training domain into training and validation subsets, and takes the sum of the validated risks over the training domains. Obviously, this is not an estimate of the o.o.d. risk. LOD-CV holds out one domain among the training domains in turn and validates models with the average of the validated risks over the held-out domains. Again, this average does not correspond to the o.o.d. risk. In summary, the problem we need to solve is answering the following question: how can we construct an evaluation function of the o.o.d. risk from validation data? In the sequel, we will propose two methods of CV, which are summarized in Algorithm 1.

3.2 Method I: using data of higher level task

We divide each of $\mathcal{D}^{e^*}, \mathcal{D}^{e_1}_{ad}, ..., \mathcal{D}^{e_n}_{ad}$ into K parts where $|\mathcal{E}_{ad}| = n$, and use the k-th sample $\{\mathcal{D}^{e^*}_{[k]}, \mathcal{D}^{e_1}_{ad,[k]}, ..., \mathcal{D}^{e_n}_{ad,[k]}\}$ and the rest $\{\mathcal{D}^{e^*}_{[-k]}, \mathcal{D}^{e_1}_{ad,[-k]}, ..., \mathcal{D}^{e_n}_{ad,[-k]}\}$ for validation and training, respectively. To approximate the o.o.d. risk of the trained predictor $p_{\theta^\lambda_{[-k]}} \circ \Phi^\lambda_{[-k]}$, we wish to estimate $\mathcal{R}^e(p_{\theta^\lambda_{[-k]}} \circ \Phi^\lambda_{[-k]})$ for $e \in \mathcal{E}_{ad} \cup \{e^*\}$ by the validation set. For e^*, we use the standard empirical estimate $\hat{\mathcal{R}}^{e^*}_{[k]}(p_{\theta^\lambda_{[-k]}} \circ \Phi^\lambda_{[-k]})$. For $e \in \mathcal{E}_{ad}$, we substitute unavailable Y^e with Z^e and use $\hat{\mathcal{R}}^{(X^e,Z^e)}_{[k]}(p_{\theta^\lambda_{[-k]}} \circ \Phi^\lambda_{[-k]}) := \frac{1}{|\mathcal{D}^e_{ad,[k]}|}\sum_{(x^e,z^e)\in\mathcal{D}^e_{ad,[k]}} -\log p_{\theta^\lambda_{[-k]}}(z^e|\Phi^\lambda_{[-k]}(x^e))$.

Algorithm 1 CV methods. If CORRECTION = True, λ is selected by method II and if False, I.

Require: : Split $\mathcal{D}^{e^*}, \mathcal{D}^{e_1}_{ad}, ..., \mathcal{D}^{e_n}_{ad}$ into K parts. Set the hyperparameter candidates Λ.

Require: :$\hat{P}^e(z^{\curlyvee}) \leftarrow \frac{|\mathcal{D}^e_{ad,z^{\curlyvee}}|}{|\mathcal{D}^e_{ad}|}$, where $\mathcal{D}^e_{ad,z^{\curlyvee}} := \{(x,z) \in \mathcal{D}^e_{ad} \,|z = z^{\curlyvee}\}$ for all $e \in \mathcal{E}_{ad}$ and $z^{\curlyvee} \in \mathcal{Z}^{\curlyvee}$.

for $\lambda \in \Lambda$ **do**
  for $k = 1$ to K **do**
    Learn $\theta^{\lambda}_{[-k]}, \Phi^{\lambda}_{[-k]}$ by using $\mathcal{D}^{e^*}_{[-k]}, \mathcal{D}^{e_1}_{ad,[-k]}, ..., \mathcal{D}^{e_n}_{ad,[-k]}$.
    $\hat{\mathcal{R}}^{e^*}_k(\lambda) \leftarrow \frac{1}{|\mathcal{D}^{e^*}_{[k]}|} \sum_{(x^{e^*},y^{e^*}) \in \mathcal{D}^{e^*}_{[k]}} -\log p_{\theta^{\lambda}_{[-k]}}(y^{e^*}|\Phi^{\lambda}_{[-k]}(x^{e^*}))$ //Risk estimation on e^*.
    $\hat{\mathcal{R}}^{e^*|z^{\curlyvee}}_k(\lambda) \leftarrow \frac{1}{|\mathcal{D}^{e^*}_{[k],z^{\curlyvee}}|} \sum_{(x,y) \in \mathcal{D}^{e^*}_{[k],z^{\curlyvee}}} -\log p_{\theta^{\lambda}_{[-k]}}(y|\Phi^{\lambda}_{[-k]}(x), g(Y) = z^{\curlyvee})$ for $z^{\curlyvee}$ in $\mathcal{Z}^{\curlyvee}$.
    for $e \in \mathcal{E}_{ad}$ **do**
      $\hat{\mathcal{R}}^e_k(\lambda) \leftarrow \frac{1}{|\mathcal{D}^e_{ad,[k]}|} \sum_{(x^e,z^e) \in \mathcal{D}^e_{ad,[k]}} -\log p_{\theta^{\lambda}_{[-k]}}(z^e|\Phi^{\lambda}_{[-k]}(x^e))$. // Risk estimation on e.
      if CORRECTION **then**
        $\hat{\mathcal{R}}^e_k(\lambda) \; + \leftarrow \; \sum_{z^{\curlyvee} \in \mathcal{Z}^{\curlyvee}} \hat{P}^e(z^{\curlyvee}) \cdot \hat{\mathcal{R}}^{e^*|z^{\curlyvee}}_k(\lambda)$ // Correction term addition.
      end if
    end for
    $\hat{\mathcal{R}}^{o.o.d.}_k(\lambda) \leftarrow \max_{e \in \mathcal{E}_{ad} \cup \{e^*\}} \hat{\mathcal{R}}^e_k(\lambda)$ // o.o.d. risk estimation.
  end for
  $\hat{\mathcal{R}}^{o.o.d.}(\lambda) \leftarrow \frac{1}{K} \sum_{k=1}^{K} \hat{\mathcal{R}}^{o.o.d.}_k(\lambda)$ // Final o.o.d. risk estimation.
end for
Select $\lambda^* := \mathrm{argmin}_{\lambda \in \Lambda} \hat{\mathcal{R}}^{o.o.d.}(\lambda)$

3.3 Method II: using correction term

Method I can be improved by correcting the replacement $\mathcal{R}^e = \mathcal{R}^{(X^e,Y^e)}$ with $\mathcal{R}^{(X^e,Z^e)}$ for $e \in \mathcal{E}_{ad}$. We use the following theorem for the correction:

Theorem 2. *Let $\mathcal{Z}^{\curlyvee} := \left\{z \in \mathcal{Z} \,\middle|\, |g^{-1}(z)| > 1\right\}$. For any map $\Phi : \mathcal{X} \to \mathcal{H}$, $p_\theta : \mathcal{H} \to \mathcal{P}_{\mathcal{Y}}$, and random variable (X,Y) on $\mathcal{X} \times \mathcal{Y}$, the following equality holds:*

$$\mathcal{R}^{(X,Y)}(p_\theta \circ \Phi) = \mathcal{R}^{(X,g(Y))}(p_\theta \circ \Phi) + \sum_{z^{\curlyvee} \in \mathcal{Z}^{\curlyvee}} \Big\{ P(g(Y) = z^{\curlyvee}) \times \mathcal{R}^{(X,Y)|z^{\curlyvee}}(p_\theta \circ \Phi) \Big\}.$$

Here, $\mathcal{R}^{(X,Y)|z^{\curlyvee}}(p_\theta \circ \Phi) := \int -\log p_\theta\big(Y|\Phi(X), g(Y) = z^{\curlyvee}\big) dP_{(X,Y)|g(Y)=z^{\curlyvee}}$ where $P_{(X,Y)|g(Y)=z^{\curlyvee}}$ denotes the conditional distribution of (X,Y) given the event $g(Y) = z^{\curlyvee}$, and $p_\theta(y|\Phi(x), g(Y) = z^{\curlyvee}) := \frac{p_\theta(y|\Phi(x))}{\sum_{y \in g^{-1}(z^{\curlyvee})} p_\theta(y|\Phi(x))}$.

The proof is given in Appendix A. The theorem shows that, to estimate the correction term, we need to estimate (i)$P(g(Y^e) = z^{\curlyvee})$ and (ii) $\mathcal{R}^{(X^e,Y^e)|z^{\curlyvee}}(p_{\theta^{\lambda}_{[-k]}} \circ \Phi^{\lambda}_{[-k]})$ for every $z^{\curlyvee} \in \mathcal{Z}^{\curlyvee}$.

(i) is naturally estimated even on $e \in \mathcal{E}_{ad}$: $\hat{P}(Z^e = z^{\curlyvee}) := \frac{|\mathcal{D}^e_{ad,z^{\curlyvee}}|}{|\mathcal{D}^e_{ad}|}$, where $\mathcal{D}^e_{ad,z^{\curlyvee}} := \{(x,z) \in \mathcal{D}^e_{ad} \,|z = z^{\curlyvee}\}$. (ii) is not easily estimable; while a direct simulation of the integration $\int dP_{(X^e,Y^e)|g(Y^e)=z^{\curlyvee}}$ demands data from $(X^e,Y^e) \sim P_{X^e,Y^e}$, our available data $\mathcal{D}^e_{ad}$ on $e \in \mathcal{E}_{ad}$ is from $P_{X^e,g(Y^e)}$, not from P_{X^e,Y^e}. To solve the non-availability of data from P_{X^e,Y^e}, we use the training data $\mathcal{D}^{e^*} \sim P_{X^{e^*},Y^{e^*}}$ instead. Namely, (ii) is estimated by

$$\hat{\mathcal{R}}^{(X^{e^*},Y^{e^*})|z^{\curlyvee}}_{[k]}(p_{\theta^{\lambda}_{[-k]}} \circ \Phi^{\lambda}_{[-k]}) := \frac{1}{|\mathcal{D}^{e^*}_{[k],z^{\curlyvee}}|} \sum_{(x,y) \in \mathcal{D}^{e^*}_{[k],z^{\curlyvee}}} -\log p_{\theta^{\lambda}_{[-k]}}(y|\Phi^{\lambda}_{[-k]}(x), g(Y) = z^{\curlyvee}),$$

where $\mathcal{D}^{e^*}_{[k],z^{\curlyvee}} := \left\{(x,y) \in \mathcal{D}^{e^*}_{[k]} \,|g(y) = z^{\curlyvee}\right\} \subset \mathcal{D}^{e^*}_{[k]}$. In Algorithm 1, the above risk estimate is abbreviated by $\hat{\mathcal{R}}^{e^*|z^{\curlyvee}}_{[k]}(\lambda)$ for notation simplicity.

4 Theoretical analysis

Throughout this section, to avoid discussing the non-trivial effects of nonlinear Φ, we focus on the simplified case of variable selections, where the feature map Φ is chosen from the projections of x

to a subset of its components. For example, Φ may be $\Phi(x_1, x_2, x_3) = (x_1, x_3)$ when x is three-dimensional. This type of IL appears practically in causal inference [14, 13] and regression [40]. Let $\mathcal{X} := \mathcal{X}_1 \times \mathcal{X}_2$ where $\mathcal{X}_1 := \mathbb{R}^{n_1}$ and $\mathcal{X}_2 := \mathbb{R}^{n_2}$ with $n_1, n_2 \in \mathbb{N}$. For a projection Φ, let Φ_i denote the $\mathcal{X}_i$-component of Φ ($i = 1, 2$). If Φ has a $\mathcal{X}_2$-component, we write $\mathrm{Im}\Phi_2 \neq \emptyset$. For simplicity of analysis, the domain set $\mathcal{E}$ is defined by all the probability distributions with the fixed marginal distribution $P_{X_1^I, Y^I}$ of (X_1, Y); namely,

$$\{(X^e, Y^e)\}_{e \in \mathcal{E}} := \left\{ (X, Y) : \text{a random variable on } \mathcal{X} \times \mathcal{Y} \,\middle|\, P_{\Phi^{\mathcal{X}_1}(X), Y} = P_{X_1^I, Y^I} \right\}. \qquad (※)$$

In this case, for any $e \in \mathcal{E}$ the variable (X^e, Y^e) satisfies (i) $P_{Y^e|\Phi^{\mathcal{X}_1}(X^e)}$ equals to $P_{Y^I|X_1^I}$, and (ii) the marginal distribution $P_{\Phi^{\mathcal{X}_1}(X)}$ of the invariant feature $\Phi^{\mathcal{X}_1}(X)$ equals to $P_{X_1^I}$. The above setting and definition persist through Section 4.

4.1 Theoretical analysis of our objective function

The following theorem ensures that, neglecting estimations and under some conditions, a minimum of our objective function (5) with careful hyperparameter choice also minimizes the o.o.d. risk (1):

Theorem 3 (o.o.d. optimality of our objective function)**.** *Under the setting (※), additionally assume that the following condition holds:*

(A) For any variable selection Φ with $\mathrm{Im}\Phi_2 \neq \emptyset$, there exist two domains $\{e_1, e_2\} \subset \mathcal{E}_{ad}$ such that $P(g(Y^{e_1})|\Phi(X^{e_1})) \neq P(g(Y^{e_2})|\Phi(X^{e_2}))$.

Then, there exists $\lambda^* \in \mathbb{R}$ such that any minimizer $(\theta^\dagger, \theta^\dagger_{ad}, \Phi^\dagger)$ of (5),

$$(\theta^\dagger, \theta^\dagger_{ad}, \Phi^\dagger) \in \operatorname*{argmin}_{\theta, \theta_{ad}, \Phi} \{ \mathcal{R}^{e^*}(p_\theta \circ \Phi) + \lambda^* \cdot \sum_{e \in \mathcal{E}_{ad}} \| \nabla_{\hat{\theta}_{ad} = \theta_{ad}} \mathcal{R}^{(X^e, Z^e)}(p^{\mathcal{Z}|\mathcal{H}}_{\hat{\theta}_{ad}} \circ \Phi) \|^2 \},$$

is o.o.d. optimal, i.e.,

$$p_{\theta^\dagger} \circ \Phi^\dagger \in \operatorname{argmin}_{p_\theta : \mathcal{X} \to \mathcal{P}_\mathcal{Y}} \mathcal{R}^{o.o.d.}(p_\theta),$$

where models p_θ and $p^{\mathcal{Z}|\mathcal{H}}_{\theta_{ad}}$ in $\min_{\theta, \theta_{ad}, \Phi}$ run all the probability density functions, and Φ runs all the variable selections. The gradient $\nabla_{\theta_{ad}}$ should be understood as the functional derivative on the space of probability density functions.

For the proof, see Appendix B. Condition (A) means that $\mathcal{E}_{ad}$ has sufficient variation to capture the desirable invariance $\Phi^{\mathcal{X}_1}$.

4.2 Theoretical analysis of our cross validation methods

In Sections 3.2 and 3.3, we approximate $\mathcal{R}^{(X^e, Y^e)}$ using label Z^e of higher level. While the approximation is not exact, we will prove that the proposed CV methods still select a correct hyperparameter under some conditions. We will also elucidate the difference of the two CV methods. Given hyperparameter λ, minimizing (5) over the model yields the feature map (variable selection) denoted by $\Phi^\lambda : \mathcal{X} \to \mathbb{R}^{n_\lambda}$ ($n_\lambda \leq n_1 + n_2$). For simplicity of theoretical analysis, we assume that the minimization of (5) achieves perfectly the conditional probability density function of $P_{Y^{e^*}|\Phi^\lambda(X^{e^*})}$, denoted by $p^{*,\lambda}(y|\Phi^\lambda(x))$. Then, neglecting estimation errors, the approximated o.o.d. risk of $p^{*,\lambda} \circ \Phi^\lambda$ used in Methods I and II are represented by the following $\mathcal{R}^I(\lambda)$ and $\mathcal{R}^{II}(\lambda)$, respectively:

$$\mathcal{R}^I(\lambda) := \max \left\{ \max_{e \in \mathcal{E}_{ad}} \mathcal{R}^{(X^e, g(Y^e))}(p^{*,\lambda} \circ \Phi^\lambda), \mathcal{R}^{(X^{e^*}, Y^{e^*})}(p^{*,\lambda} \circ \Phi^\lambda) \right\},$$

$$\mathcal{R}^{II}(\lambda) := \max_{e \in \mathcal{E}_{ad} \cup \{e^*\}} \left\{ \mathcal{R}^{(X^e, g(Y^e))}(p^{*,\lambda} \circ \Phi^\lambda) + \sum_{z^\curlyvee \in \mathcal{Z}^\curlyvee} P(Z^e = z^\curlyvee) \cdot \mathcal{R}^{(X^{e^*}, Y^{e^*})|z^\curlyvee}(p^{*,\lambda} \circ \Phi^\lambda) \right\}.$$

We have the following theoretical justification of our CV methods: the chosen λ gives a minimizer of the correct CV criterion. For the proofs, see Appendices C and D.

Theorem 4 (Correctness of Method I)**.** *Assume that the following conditions (i) and (ii) hold:*

(i) Among a set Λ of hyperparameter candidates, there exists $\lambda^I \in \Lambda$ such that $\Phi^{\lambda^I} = \Phi^{\mathcal{X}_1}$.

(ii) Let p^{e^*} be the probability density function of $P_{X^{e^*},g(Y^{e^*})}$. Then, for any λ with $\mathrm{Im}\Phi_2^\lambda \neq \emptyset$, there is $e_\lambda \in \mathcal{E}_{ad}$ such that

$$(x,z) \sim P_{X^{e_\lambda},g(Y^{e_\lambda})} \text{ satisfies } p^{e^*}(z|\Phi^\lambda(x)) \leq e^{-\beta} - \varepsilon \text{ with probability 1.}$$

Here, $\varepsilon \in \mathbb{R}_{>0}$ is some sufficient small positive real number (that is, $0 < \varepsilon \ll 1$) and $\beta := H(Y^{e^*}|\Phi^{\mathcal{X}_1}(X^{e^*}))$ is the conditional entropy of $(\Phi^{\mathcal{X}_1}(X^{e^*}), Y^{e^*})$.

Then, under the setting (※), we have

$$\mathrm{argmin}_{\lambda\in\Lambda}\, \mathcal{R}^I(\lambda) \subset \mathrm{argmin}_{\lambda\in\Lambda}\, \mathcal{R}^{o.o.d.}(p^{*,\lambda} \circ \Phi^\lambda).$$

Theorem 5 (Correctness of Method II)**.** *Assume that, in addition to (i) in Theorem 4, the following condition (iii) holds:*

(ii)' for any λ with $\mathrm{Im}\Phi_2^\lambda \neq \emptyset$, there is $e_\lambda \in \mathcal{E}_{ad}$ such that

$$(x,z) \sim P_{X^{e_\lambda},g(Y^{e_\lambda})} \text{ satisfies } p^{e^*}(z|\Phi^\lambda(x)) \leq e^{-\beta_\lambda} - \varepsilon \text{ holds with probability 1.}$$

Here, ε is some sufficiently small positive real number and

$$\beta_\lambda := H(Y^{e^*}|\Phi^{\mathcal{X}_1}(X^{e^*})) - \sum_{z^{\checkmark} \in \mathcal{Z}^{\checkmark}} \left\{ P(g(Y^{e^*}) = z^{\checkmark}) \times \mathcal{R}^{(X^{e^*},Y^{e^*})|z^{\checkmark}}(p^{*,\lambda} \circ \Phi^\lambda) \right\}.$$

Then, under the setting (※), we have

$$\mathrm{argmin}_{\lambda\in\Lambda}\, \mathcal{R}^{II}(\lambda) \subset \mathrm{argmin}_{\lambda\in\Lambda}\, \mathcal{R}^{o.o.d.}(p^{*,\lambda} \circ \Phi^\lambda).$$

The conditions (ii) and (ii)' impose that, for at least one $e_\lambda \in \mathcal{E}_{ad}$, the two domains e_λ and e^* are *different* in the following meaning. if λ fails to remove domain-specific factors ($i.e.$, $\mathrm{Im}\Phi_2^\lambda \neq \emptyset$), for some $e_\lambda \in \mathcal{E}_{ad}$, $(x,z) \sim P_{X^{e_\lambda},g(Y^{e_\lambda})}$ yields low $p^{e^*}(z|\Phi^\lambda(x))$ with high probability. On the other hand, $(x,z) \sim P_{X^{e^*},g(Y^{e^*})}$ yields high $p^{e^*}(z|\Phi^\lambda(x))$ with high probability: that is, e^* and e_λ are *different*.

The theoretical analysis shows, while Method I is simpler to implement than Method II, Method II is more applicable. Noting that $\beta \geq \beta_\lambda$ and hence, $e^{-\beta} - \varepsilon \leq e^{-\beta_\lambda} - \varepsilon$, the condition (ii)' is milder than (ii). Recalling that (ii) and (ii)' impose the discrepancy between $\mathcal{E}_{ad}$ and e^* as discussed in the last paragraph, relaxation of conditions from (ii) to (ii)' implies that *method II can be applied even when domains $\mathcal{E}_{ad}$ and e^* have smaller discrepancy than the condition for Method I.* The difference of these two methods will be demonstrated in Section 6. The real-world feasibility of the assumptions (ii) and (ii)' are discussed in Appendix F.

5 Related work

Fine-tuning The proposed framework uses additional data from multiple domains as well as the training data for the target task. It is relevant to Transfer learning (TL) [22–24] and meta-learning [30, 41], which realize fast and accurate learning for a new target task based on a model pre-trained with additional data sets. For example, after initial learning with a large data set, *fine tune* [22, 23] re-trains the model with the target task, while *frozen feature* [24] fixes the pre-trained model and tunes a head network. Although they show advantages in many learning problems, they may not work effectively in the current setting; in the fine-tuning with the target task (X^{e^*}, Y^{e^*}), the model tends to learn biased correlation in the data set and does not generalize to unseen domains. Some fine-tuning methods will be compared with the proposed approach in Section 6.

Domain adaptation by deep feature learning Domain adaptation strategies by deep feature learning [25–27, 31, 32] assume that we can access input data on a test domain in advance, and try to obtain data representation $\Phi(X^e)$ that follows the same distribution for the training and test domains. While the strategies lead to high predictive performance on a test domain similar to a training domain, such Φ does not function by discarding environmental factors from $X^e \in \mathcal{X}$ as noted in [10]. Experimental comparisons will be shown in Section 6.

Distributionally robust optimizations and other debias methods are discussed in Appendix G.

6 Experiments

We study the effectiveness of the proposed framework and CVs through experiments, comparing them with several existing methods: empirical risk minimization (ERM), fine-tuning methods, and

Dataset	CMNIST	ImageNet $\mathcal{Y} = [3]$	ImageNet $\mathcal{Y} = [7]$	ImageNet $\mathcal{Y} = [17]$,
Best possible	.750			
random guess	.100	.333	.143	.059
Oracle	.715 (.001)	.743 (.018)	.749 (.008)	.708 (.010)
ERM	.433 (.004)	.417 (.016)	.507 (.020)	.357 (.020)
FT	.250 (.020)	.463(.030)	.409 (.020)	.361 (.011)
FF	.248 (.019)	.482 (.127)	.226 (.046)	.162 (.011)
DSAN	.073 (.003)	.278 (.004)	.293 (.008)	.060 (.007)
Ours + CV I	.606 (.051)	.652 (.028)	**.622 (.011)**	**.556 (.004)**
Ours + CV II	**.618 (.018)**	**.666 (.027)**	**.622 (.011)**	**.556 (.004)**
Ours + Tr-CV	.500 (.006)	.641 (.033)	.612 (.012)	.544 (.013)
Ours + LOD CV	.460 (.200)	.525(.028)	.572 (.022)	.528 (.019)
Ours + TDV	.657 (.008)	.673 (.035)	.634 (.033)	.556 (.004)

Table 1: Average Test Accuracies and SEs of Colored MNIST and ImageNet (5 runs): *Oracle* show the result of ERM with grayscale MNIST (CMNIST) and of training with both e_1 and e_2 (ImageNet). TDV selects λ that yields the highest performance on e_2. The best scores are **bolded**.

Dataset	CVI	CVII	Tr-CV	LOD-CV
CMNIST	.051 (.053)	**.039 (.017)**	.163 (.006)	.197 (.205)
ImageNet: $\mathcal{Y} = [3]$	.027 (.029)	**.013 (.020)**	.025 (.021)	.170 (.041)
ImageNet: $\mathcal{Y} = [7]$	**.012 (.001)**	**.012 (.001)**	.018 (.015)	.054 (.024)
ImageNet: $\mathcal{Y} = [17]$	**.000 (.000)**	**.000 (.000)**	.001 (.002)	.025 (.021)

Table 2: Means and SEs of $\{$(Accuracy of TDV on e_2) $-$ (Accuracy of Each CV on e_2) $\}$ (5runs). The lowest errors are **bolded**.

deep domain adaptation strategies. For fine-tuning, we employ two typical methods of transfer learning: *fine tune* (FT) and *frozen feature* (FF) [22–24]. As a deep domain adaptation technique, we adopt the state-of-the-art method $DSAN$ [31]. We also compare our two CVs (CVI and CVII) with conventional CVs: training-domain validation (Tr-CV) and leave-one-domain-out cross-validation (LOD-CV) [19]. We have two hyperparameters to be selected by CV. In the training with (5), we set $\lambda := \lambda_{\text{before}}$ when the training epoch is less than a certain threshold t, and $\lambda := \lambda_{\text{after}}$ if the epoch is larger than t. It is known that these two hyperparameters are critical for IL methods to achieve good results. From a set of candidates, each of the CV methods selects a pair $(t, \lambda_{\text{after}})$. To know the best possible performance among the candidates, we also apply the test-domain validation (TDV) [19], which selects the hyperparameters with the unseen test domain, and thus is not applicable in practical situations. Additional experiments and experimental details can be found in Appendices H and I, respectively. The code is available in Supplementary Material.

Colored MNIST We apply our framework to *Colored MNIST* [10] with $\mathcal{Y} = [10]$ and $\mathcal{Z} := [2]$. We aim to predict $Y^e \in \mathcal{Y}$ from digit image data $X^e \in \mathbb{R}^{2\times 24\times 24}$. The label Y^e is changed randomly to one of the rest uniformly with a probability of 25%. All digits in images are colored red or green. The domain $e \in [0, 1]$ controls the color of digits; the digits $Y^e > 4$ and $Y^e \leq 4$ are colored in red and green, respectively, with probability e. In training, $\mathcal{D}^{e^*} \sim P_{X^{0.1}, Y^{0.1}}$ is drawn with sample size $n^{e^*} = 5000$, and in testing, Y^e is predicted from X^e for $e_2 := 0.9$. Regarding the higher level Z^e, the task is to predict $Z^e = 0$ for X^e in $0 - 4$ and $Z^e = 1$ for $5 - 9$ (that is, $g(Y^e) = 1$ if $Y^e > 4$ and else, $g(Y^e) = 0$). The label Z^e is swapped randomly with 25%. We set $\mathcal{E}_{ad} = \{0.1, 0.3, 0.5, 0.7, 0.9\}$ with $n^e = 5000$ for each $e \in \mathcal{E}_{ad}$. We model Φ by a 3-layer neural net. Setting the maximum epoch 500 and $\lambda_{\text{before}} := 1.0$, we select $(t, \lambda_{\text{after}})$ from 4×7 candidates with $t \in \{0, 100, 200, 300\}$, $\lambda_{\text{after}} \in \{10^0, 10^1, ..., 10^6\}$ by each of the CVs.

Table 1 shows the test accuracies for 2000 random samples in the domain e_2. The results, together with additional ones in Appendices H.1 and H.2, demonstrate that the proposed methods significantly outperform the others for e_2. Among the two proposed methods, CV II yields higher test accuracies on e_2. Table 2 shows the accuracy gain of each CV from TDV with the same data sets for domain e_2. These results, together with Appendices H.1 and H.2, concur with the theory in Section 4 suggesting that CVII succeeds in wider situations, resulting in smaller errors.

ImageNet To see the performance of the proposed methods for more practical data, they are applied to the ImageNet [53] with its label re-annotated imitating BREEDS [52], which proposes a

method for re-annotating ImageNet to create an o.o.d. benchmark. The target task here is to predict labels $Y^e \in \mathcal{Y}$ of images $X^e \in \mathbb{R}^{3\times 224\times 224}$. We conduct three experiments with $|\mathcal{Y}| = 3, 7, 17$. For each experiment, we prepare image datasets in different two manners e_1 and e_2. 2, 4 and 8 classes out of 3, 7 and 17 classes, respectively, are composed of different subtypes between e_1 and e_2; for example, the images of class *bird* in e_1 are composed of ruffed grouse and indigo bunting, and the bird images on e_2 are composed of albatross and water ouzel (Figure 2). In detail, show Appendix I.3. In training, $\mathcal{D}^{e^*} \sim P_{X^{e_1},Y^{e_1}}$ is drawn, and in testing, Y^e is predicted from X^e on e_2. The coarser label Z^e is binary (that is, $\mathcal{Z} = [2]$), and the sample in the higher level $\mathcal{D}^e_{ad}$ of (X^e, Z^e) is drawn from both e_1 and e_2. Here, $\mathcal{D}^{e_1}_{ad}$ is the same as $\mathcal{D}^{e^*}$ but with labels re-annotated by g. We model Φ by ResNet50 [29]. Setting the maximum epoch 32 and $\lambda_{\text{before}} := 0.1$, we select $(t, \lambda_{\text{after}})$ from 3×4 candidates with $t \in \{10, 20, 30\}$, $\lambda_{\text{after}} \in \{0, 1, 10, 100\}$ by each of the CVs.

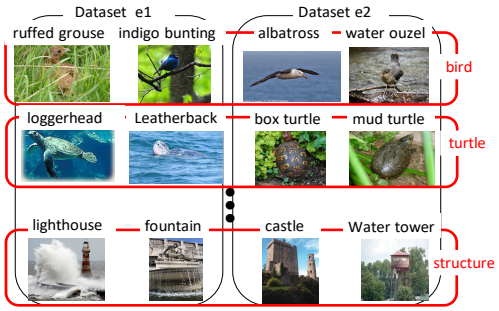

Figure 2: ImageNet experiment dataset.

Table 1 shows the test accuracies on e_2. We can see that the proposed framework succeeded in capturing the predictor invariant to the change of e, while the other methods failed. Table 2, which shows the difference between accuracies by TDV and each CV for the same data set with e_2, verify that CVI and II selects λ with the smallest error.

Comparison of two CV methods To highlight the difference between the proposed two CVs, we compare them regarding the discrepancy between the additional domains of higher level $\mathcal{E}_{ad}$ and the domain for training of the target task e^*. We used synthesized data with $\mathcal{X} = \mathbb{R}^2$, $\mathcal{Y} = [10]$ and $\mathcal{Z} := [2]$, preparing ten distributions $\{N_i\}_{i=1}^{10}$ on $\mathbb{R}^2$, which include a domain-specific factor in the second component depending on $e \in \mathbb{Z}$ (see Appendix I.2 for explicit representations of $\{N_i\}_{i=1}^{10}$). The task is to predict the distribution label $i \in \{1, \ldots, 10\}$. Setting $e^* := 20$ with $n^{e^*} = 60000$, the test task is to predict the label for domain $e = -20$. Regarding the task with label of higher level, we use $g(y) = 0$ if $y > 4$ and $g(y) = 0$ else. We draw $\mathcal{D}^e_{ad} \sim P_{X^e,Z^e}$ ($n^e = 20000$) from $\mathcal{E}_{ad} = \{e_{ad}, 40\}$, where e_{ad} ranges from -9 to 1. As e_{ad} increases, e_{ad} approaches to e^*. The model Φ is a 3-layer neural net. We set the maximum epoch 500 and $t = 0$, and select λ_{after} from 4 candidates $\lambda_{\text{after}} \in \{0, 0.001, 80, 100\}$ by each CV method.

	$e_{ad} = -9$	$e_{ad} = -8$	$e_{ad} = -7$	$e_{ad} = -6$	$e_{ad} = -5$	$e_{ad} = -4$	$e_{ad} = -3$	$e_{ad} = -2$	$e_{ad} = -1$	$e_{ad} = 0$	$e_{ad} = 1$
TDV	.596 (.078)	.621 (.046)	.630 (.041)	.595 (.061)	.590 (.087)	.621 (.059)	.564 (.071)	.582 (.056)	.535 (.093)	.520 (.121)	.575 (.107)
CV I	**.529 (.128)**	.555 (.111)	.562 (.086)	.566 (.109)	.375 (.145)	.346 (.172)	.372 (.176)	.358 (.167)	.300 (.146)	.173 (.143)	.218 (.087)
CV II	.527 (.152)	**.573 (.089)**	**.565 (.085)**	**.572 (.072)**	**.522 (.110)**	**.523 (.102)**	**.482 (.113)**	**.506 (.153)**	**.430 (.146)**	**.437 (.157)**	**.502 (.149)**

Table 3: Comparison of Two CVs: Average Test ACCs and SEs of the estimates (10runs).

Table 3 shows the test accuracy on $e = -e^*$ with 2000 random samples $(x, y) \sim P_{X^{-e^*},Y^{-e^*}}$. From the results, we can see that CVII tends to select better hyperparameters than CVI, especially in the case where the variation among the domains is smaller as e_{ad} approaches to e^*. This accords with the theoretical results in Theorems 4 and 5, which show that CVII finds a correct hyperparameter in smaller discrepancy between $\mathcal{E}_{ad}$ and e^* than CVI.

7 Conclusion

We have proposed a new framework of invariance learning: assuming the availability of datasets for another relevant task in higher label hierarchy, we obtain an invariant predictor for the target classification task using training data in a *single* domain. We have also proposed two CV methods for hyperparameter selection, which has been an outstanding problem of previous methods for invariant learning. Theoretical analysis has revealed correctness of our methods, including CVs, and the experimental results have demonstrated the effectiveness of the proposed framework and CVs.

Limitations and Potential societal impact In Theorem 3, it is ensured that our objective function gives a minimizer of the o.o.d. risk, only if at least two domains have a discrepancy concerning distributions. In general, different domains have different distributions. Judging the discrepancy is a further important problem. As a positive impact, our method will enable us to estimate predictors that don't use discriminatory factors such as gender. There may be some negative aspects in that our method removes important information for a prediction as well as unnecessary ones.

References

[1] V. Vapnik. Principles of risk minimization for learning theory. *In NIPS*, 1992.

[2] L. Adolphs, J. Kohler, and A. Lucchi. Ellipsoidal trust region methods and the marginal value of Hessian information for neural network training. *arXiv:1905.09201 (version 1)*, 2019.

[3] S. Beery, G. V. Horn, P. Perona. Recognition in terra incognita. *In ECCV*, 2019.

[4] J. R. Zech, M.A. Badgeley, M. Liu, A. B. Costa, J. J. Titano, E. K. Oermann. Variable generalization performance of a deep learning model to detect pneumonia in chest radiographs: A cross-sectional study. *PLoS Medicine 15, e1002683* , 2018.

[5] T. Niven, H.-Y Kao. Probing neural network comprehension of natural language arguments. *Proceedings of the 57th Annual Meeting of the Association for Computational*, 2019.

[6] S. Gururangan, S. Swayamdipta, O. Levy, R. Schwartz, S. R. Bowman, N. A. Smith. Annotation artifacts in Natural Language Inference data. *Proceedings of the Conference of the North American Chapter of the Association for Computational Linguistics*, 2018.

[7] J. Dastin. Amazon scraps secret AI recruiting tool that showed bias against women. *https://reut.rs/2Od9fPr*, 2018.

[8] A. Ilyas, S. Santurkar, D. Tsipras, L. Engstrom, B. Tran, A. Madry. Adversarial examples are not bugs, they are features. *In NeurIPS*, 2019.

[9] J. Shane. Do neural nets dream of electric sheep? *https://aiweirdness.com/post/171451900302/* , 2018.

[10] M. Arjovsky, L. Bottou, I. Gulrajani, and D. Lopez-Paz. Invariant Risk Minimization. *arXiv:1907.02893*, 2019.

[11] K. Ahuja, K. Shanmugam, K. Varshney, and A. Dhurandhar. Invariant risk minimization games. *In ICML*, 2020.

[12] D. Rothenhausler, P. Buhlmann, N. Meinshausen, and J. Peters. Anchor regression: heterogeneous data meets causality. *JRSS B*, 83(2):215–246, 2018.

[13] C. Heinze-Deml, J. Peters, and N. Meinshausen. Invariant causal prediction for nonlinear models. *Journal of Causal Inference*, 6(2), 2018.

[14] J. Peters, P. Bühlmann, and N. Meinshausen. Causal inference using invariant prediction: identification and confidence intervals. *JRSS B,* 6(2): 947-1012, 2016.

[15] M. Koyama, S. Yamaguchi. When is invariance useful in an Out-of-Distribution Generalization problem? *arXiv*, 2008.01883, 2020.

[16] E. A. AlBadawy, A. Saha, and M. A. Mazurowski. Deep learning for segmentation of brain tumors: Impact of cross-institutional training and testing. *Medical physics,* 45(3): 1150-1158, 2018.

[17] C. S. Perone, P. Ballester, R. C. Barros, and J. Cohen-Adad. Unsupervised domain adaptation for medical imaging segmentation with self-ensembling. *NeuroImage*, 194(1): 1-11, 2019.

[18] W. D. Heaven. Google's medical AI was super accurate in a lab. real life was a different story. *MIT Technology Review,* 2020.

[19] I. Gulrajani, D. Lopez-Paz. In Search of Lost Domain Generalization. *In ICLR,* 2021.

[20] P. Kamath. Does Invariant Risk Minimization Capture Invariance? *In AISTATS,* 2021.

[21] D. Krueger, E. Caballero, J. Jacobsen, A. Zhang, J. Binas, D. Zhang, R. L. Priol, A. Courville. Out-of-Distribution Generalization via Risk Extrapolation. *In ICML,* 2021.

[22] S. J. Pan, and Q. Yang. A survey on transfer learning. *IEEE Transactions on Knowledge and Data Engineering* , 22(10):1345-1359, 2009.

[23] Q. Yang, Y. Zhang, W. Dai, and S. J. Pan. Transfer Learning. *Cambridge University Press*, 2020.

[24] J. Yosinski, J. Clune, Y. Bengio, and H. Lipson. How transferable are features in deep neural networks? *In NIPS,* 2014.

[25] Y. Ganin, E. Ustinova, H. Ajakan, P. Germain, H. Larochelle, F. Laviolette, M. March, and V. Lempitsky. Domain-adversarial training of neural networks. *Journal of Machine Learning Research*, 17(59):1-35, 2016.

[26] S. Ben-David, J. Blitzer, K. Crammer, and F. Pereira. Analysis of representations for domain adaptation. *In NIPS*, 2007.

[27] G. Louppe, M. Kagan, and K. Cranmer. Learning to pivot with adversarial networks. *In NIPS*, 2017.

[28] S. Sagawa, P. W. Koh, T. B. Hashimoto, P. Liang. Distributionally Robust Neural Networks for Group Shifts: On the Importance of Regularization for worst-case generalization. *In ECCV*, 2019.

[29] K. He, X. Zhang, S. Ren, and J. Sun. Deep residual learning for image recognition. *In CVPR*, 2016.

[30] C. Finn, P. Abbeel, and S. Levine. Model-agnostic meta- learning for fast adaptation of deep networks. *In ICML*, 2017.

[31] P. Stojanov, Z. Li, M. Gong, Ruichu Cai, J. G. Carbonell, K. Zhang. Domain Adaptation with Invariant Representation Learning: What Transformations to Learn? *In NeurIPS*, 2021.

[32] Y. Zhang, H. Tang, K. Jia, M. Tan. Domain-Symmetric Networks for Adversarial Domain Adaptation. *In CVPR*, 2019.

[33] J. Liu, Z. Hu, P. Cui, B. Li, Z. Shen. Heterogeneous Risk Minimization. *In ICML*, 2021.

[34] J. Liu, Z. Hu, P. Cui, B. Li, Z. Shen. Kernelized Heterogeneous Risk Minimization. *In NeurIPS*, 2021.

[35] J. Creager, J. Jacobsen, R. Zemel. Environment Inference for Invariant Learning. *In ICML*, 2021.

[36] G. Parascandolo, A. Neitz, A. Orvieto, L. Gresele, B. Scholkopf. Learning explanations that are hard to vary. *In ICLR*, 2021.

[37] D. P. Kingma, J. L. Ba. Adam: A Method for Stochastic Optimization. *In ICLR*, 2015.

[38] C. Wah, S. Branson, P. Welinder, P. Perona, and S. Belongie. The Caltech-UCSD Birds-200-2011 dataset. Technical report, California Institute of Technology, 2011.

[39] B. Zhou, A. Lapedriza, A. Khosla, A. Oliva, and A. Torralba. Places: A 10 million image database for scene recognition. *IEEE Transactions on Pattern Analysis and Machine Intelligence*, 40(6): 1452–1464, 2017

[40] M. Rojas-Carulla, B. Scholkopf, R. Turner, and J. Peters. Invariant models for causal transfer learning. *Journal of Machine Learning Research*, 19(36):1-34, 2018

[41] M. Andrychowicz1, M. Denil1, S. Colmenarejo1, M. W. Hoffman1, D. Pfau1, T. Schaul, B. Shillingford, N. de Freitas. Learning to learn by gradient descent by gradient descent. *In NIPS*, 2016

[42] H. Pham, Z. Dai, Q. Xie, Q. V. Le. Meta Pseudo Labels. *In CVPR*, 2021

[43] D. Lee. Pseudo-Label : The Simple and Efficient Semi-Supervised Learning Method for Deep Neural Networks. *In ICML Workshop*, 2013

[44] Z, Zheng, L. Zheng, Y. Yang. Unlabeled Samples Generated by GAN Improve the Person Reidentification Baseline in vitro. *In ICCV*, 2017

[45] X. Gu, J. Sun, Z. Xu. Spherical Space Domain Adaptation With Robust Pseudo-Label Loss. *In CVPR*, 2020

[46] T. Cour, B. Sapp, and B. Taskar. Learning from partial labels. *Journal of Machine Learning Research*, 12(42):1501-1536, 2011.

[47] Y. Yan, Y. Guo. Partial Label Learning with Batch Label Correction. *In AAAI*, 2021.

[48] N. Xu, J. Lv, X.Geng. Partial label learning via label enhancement. *In AAAI*, 2019.

[49] Y. Katsura, M. Uchida. Bridging Ordinary-Label Learning and Complementary-Label Learning. *In ACML*, 2020.

[50] L. Feng, T. Kaneko, B. Han, Ga. Niu, B. An, M. Sugiyama. Learning with Multiple Complementary Labels. *In ICML*, 2020.

[51] T. Ishida, G. Niu, A. Menon, M. Sugiyama. Complementary-Label Learning for Arbitrary Losses and Models. *In ICML*, 2019.

[52] S. Santurkar, D. Tsipras, and A. Madry. Breeds: Benchmarks for subpopulation shift. *In ICLR*, 2021.

[53] J. Deng, A. Berg, S. Satheesh, H. Su, A. Khosla, L. Fei-Fei. Imagenet: A large-scale hierarchical image database. *In CVPR*, 2009.

[54] C. Lu, Y. Wu, J. M. Hernández-Lobato, B. Scholkopf. Invariant Causal Representation Learning For out-of-distribution generalization. *In ICLR*, 2022.

[55] M. Takada, H. Fujisawa, T. Nishikawa. HMLasso: Lasso with High Missing Rate. *In IJCAI*, 2019.

[56] C. K. Enders. Imputation of missing data in industrial databases. Applied intelligence. Psychological methods, 8(3):322, 2003.

[57] K. Lakshminarayan, S. A. Harp, and T. Samad. Imputation of missing data in industrial databases. Applied intelligence, 11(3):259–275, 1999.

[58] H. Tan, G. Feng, J. Feng, W. Wang, Y. Y. J. Zhang, F. Li. A tensor-based method for missing traffic data completion. Transportation Research Part C: Emerging Technologies, 28:15–27, 2013.

[59] S. Sagawa, P. W. Koh, T. B. Hashimoto, P. Liang. Distributionally Robust Neural Networks *In ICLR*, 2020.

[60] W. Hu, G. Niu, I. Sato, and M. Sugiyama. Does distributionally robust supervised learning give robust classifiers? *In ICML*, 2018.

[61] Y. Oren, S. Sagawa, T. Hashimoto, and P. Liang. Distributionally robust language modeling. *In EMNLP*, 2019.

[62] H. Bahng, S. Chun, S. Yun, J. Choo, S. J. Oh Learning De-biased Representations with Biased Representations. *In ICML*, 2020.

[63] H, Wang, Z. Huang, H. Zhan, Y. J. Lee, E. P. Xing Toward Learning Human-aligned Cross-domain Robust Models by Countering Misaligned Features. *In UAI*, 2022.

Checklist

1. For all authors...
   (a) Do the main claims made in the abstract and introduction accurately reflect the paper's contributions and scope? [Yes]
   (b) Did you describe the limitations of your work? [Yes] In Section 1, we note that data with target classification label needs from at least one domain. In Section 4, we theoretically reveal the conditions for our objective function and CV methods to succeed.
   (c) Did you discuss any potential negative societal impacts of your work? [Yes] It is included in Section 7.
   (d) Have you read the ethics review guidelines and ensured that your paper conforms to them? [Yes]
2. If you are including theoretical results...
   (a) Did you state the full set of assumptions of all theoretical results? [Yes] See Section 4.
   (b) Did you include complete proofs of all theoretical results? [Yes] They are included in Appendices.
3. If you ran experiments...
   (a) Did you include the code, data, and instructions needed to reproduce the main experimental results (either in the supplemental material or as a URL)? [Yes] We put the code in the supplemental material.
   (b) Did you specify all the training details (e.g., data splits, hyperparameters, how they were chosen)? [Yes] They are specified in Section 6 and Appendix I.4.
   (c) Did you report error bars (e.g., with respect to the random seed after running experiments multiple times)? [Yes]
   (d) Did you include the total amount of compute and the type of resources used (e.g., type of GPUs, internal cluster, or cloud provider)? [Yes] They are included in Appendix I.4.

4. If you are using existing assets (e.g., code, data, models) or curating/releasing new assets...
   (a) If your work uses existing assets, did you cite the creators? [Yes]
   (b) Did you mention the license of the assets? [Yes]
   (c) Did you include any new assets either in the supplemental material or as a URL? [N/A]
   (d) Did you discuss whether and how consent was obtained from people whose data you're using/curating? [N/A]
   (e) Did you discuss whether the data you are using/curating contains personally identifiable information or offensive content? [N/A]
5. If you used crowdsourcing or conducted research with human subjects...
   (a) Did you include the full text of instructions given to participants and screenshots, if applicable? [N/A]
   (b) Did you describe any potential participant risks, with links to Institutional Review Board (IRB) approvals, if applicable? [N/A]
   (c) Did you include the estimated hourly wage paid to participants and the total amount spent on participant compensation? [N/A]

Supplementary Materials to "Invariance Learning based on Label Hierarchy"

A Proof of Theorem 2

$$
\begin{aligned}
\mathcal{R}^{(X,Y)}(p_\theta \circ \Phi) - \mathcal{R}^{(X,g(Y))}(p_\theta \circ \Phi) &= \int -\log p_\theta(Y|\Phi(X)) dP_{Y,\Phi(X)} \\
&\quad + \int \log p_\theta(g(Y)|\Phi(X)) dP_{g(Y),\Phi(X)} \\
&= -\int \log \frac{p_\theta(Y|\Phi(X))}{p_\theta(g(Y)|\Phi(X))} dP_{(Y,\Phi(X))} \\
&= -\int dP_{g(Y)} \int \log \frac{p_\theta(Y|\Phi(X))}{p_\theta(g(Y)|\Phi(X))} dP_{(Y,\Phi(X))|g(Y)} \qquad (6)
\end{aligned}
$$

By the definition of $p_\theta(y|\Phi(x), g(Y) = z)$ in Theorem 2, $\frac{p_\theta(y|\Phi(x))}{p_\theta(g(y)|\Phi(x))} = p_\theta(y|\Phi(x), g(Y) = z)$ holds, where $z = g(y)$. Therefore, we obtain

$$
\begin{aligned}
(6) &= -\int dP_{g(Y)} \int \log \frac{p_\theta(Y|\Phi(X))}{p_\theta(g(Y)|\Phi(X))} dP_{(Y,\Phi(X))|g(Y)} \\
&= -\int dP_{g(Y)} \int \log p_\theta(Y|\Phi(X), g(Y) = z) dP_{(Y,\Phi(X))|g(Y)=z} \\
&= -\sum_{z \in \mathcal{Z}} P(g(Y) = z) \int \log p_\theta(Y|\Phi(X), g(Y) = z) dP_{(Y,\Phi(X))|g(Y)=z} \\
&= -\sum_{z^{\not\hookrightarrow} \in \mathcal{Z}^{\not\hookrightarrow}} P(g(Y) = z^{\not\hookrightarrow}) \int \log p_\theta(Y|\Phi(X), g(Y) = z^{\not\hookrightarrow}) dP_{(Y,\Phi(X))|g(Y)=z^{\not\hookrightarrow}} \\
&\qquad + \sum_{z^{\hookrightarrow} \in \mathcal{Z} - \mathcal{Z}^{\not\hookrightarrow}} P(g(Y) = z^{\hookrightarrow}) \int \log p_\theta(Y|\Phi(X), g(Y) = z^{\hookrightarrow}) dP_{(Y,\Phi(X))|g(Y)=z^{\hookrightarrow}}. \qquad (7)
\end{aligned}
$$

Noting that, for any $z^{\hookrightarrow} \in \mathcal{Z} - \mathcal{Z}^{\not\hookrightarrow}$ and $y := g^{-1}(z^{\hookrightarrow})$[1], $p_\theta(y|\Phi(x), g(Y) = z^{\hookrightarrow}) = 1$ holds, we can see that $\log p_\theta(y|\Phi(x), g(Y) = z^{\hookrightarrow}) = 0$. The second term in the last line thus equals to zero, which concludes the proof. □

B Proof of Theorem 3

Before Proving Theorem 3, we recap the problem setting of variable selection for invariance learning discussed in the first paragraph of Section 4.

Let $\mathcal{X} := \mathcal{X}_1 \times \mathcal{X}_2$ where $\mathcal{X}_1 := \mathbb{R}^{n_1}$ and $\mathcal{X}_2 := \mathbb{R}^{n_2}$ with $n_1, n_2 \in \mathbb{N}$, so that $\mathcal{X} = \mathbb{R}^n$ with $n = n_1 + n_2$. For the class of feature map Φ, we consider the projections of $\mathcal{X}$ to a subset of variables $(x_1, \ldots, x_n)$. We have thus 2^n candidates of feature maps, and choose the best one in optimizing (5). Recall that Φ_i denote the $\mathcal{X}_i$-component of Φ $(i = 1, 2)$ and $\mathrm{Im}\Phi_2 \neq \emptyset$ means that the range of Φ has a $\mathcal{X}_2$-component.

We assume that (X_1^I, Y^I) on $\mathcal{X}_1 \times \mathcal{Y}$ gives the invariant feature X_1^I and invariant predictor $P_{Y^I|X_1^I}$. Note that the invariant features are given by $\mathcal{X}_1$ only, and the invariance learning is expected to find the projection to $\mathcal{X}_1$ as Φ. Also, we assume that the domains $\mathcal{E}$ are composed of *all* the possible distributions of X_2 with the marginal distribution of $\mathcal{X}_1 \times \mathcal{Y}$ being the same as that of (X_1^I, Y^I). Namely, we introduce the class

$$
T_{all} := \left\{ (X, Y) : \text{ random variable on } \mathcal{X} \times \mathcal{Y} \,\middle|\, P_{X_1,Y} = P_{X_1^I,Y^I} \right\}
$$

for all the domains, and often specify a domain directly by a random variable (X, Y) in T_{all}.

The training data for the target task is given by a single domain $(X^*, Y^*) \in T_{all}$. For the domains of the additional task with higher class labels, we consider a subclass $T_{ad} \subset T_{all}$. For a projection $\Phi : \mathcal{X} \to \mathbb{R}^{n_\Phi}$

[1] $z^{\hookrightarrow} \in \mathcal{Z} - \mathcal{Z}^{\not\hookrightarrow}$ implies that $|g^{-1}(z^{\hookrightarrow})| = 1$ and therefore, $g^{-1}(z^{\hookrightarrow})$ is determined uniquely. Note that there is no chance that $|g^{-1}(z^{\hookrightarrow})| = 0$ by the surjectivity of g.

with its range n_Φ variables, let $p^{*,\Phi} : \mathbb{R}^{n_\Phi} \to \mathcal{P}_\mathcal{Y}$ denote the conditional probability density functions (p.d.f.) of $P(Y^*|\Phi(X^*))$. With a slight abuse of notation, for any probability P_θ on $\mathcal{X} \times \mathcal{Y}$ and a projection Φ, the density function of the conditional distribution $P_\theta(Y|\Phi(X))$ is denoted by $p_\theta \circ \Phi$.

Throughout this section, the projection to the components of $\mathcal{X}_1$ is denoted by $\Phi^{\mathcal{X}_1}$, which is the desired projection to give the invariant predictor. From the condition of T_{all}, for the projection $\Phi^{\mathcal{X}_1}$, the conditional probability $P_{Y|\Phi^{\mathcal{X}_1}(X)}$ for *any* random variable $(X, Y) \in T_{all}$ is the same; namely, letting $p^I : \mathcal{X}_1 \to \mathcal{P}_\mathcal{Y}$ denote the conditional p.d.f. of the invariant predictor $P_{Y^I|X_1^I}$, we have

$$p^e \circ \Phi^{\mathcal{X}_1} = p^I \tag{8}$$

for any $(X^e, Y^e) \in T_{all}$, where p^e is the conditional p.d.f. of $P_{Y^e|\Phi^{\mathcal{X}_1}(X^e)}$.

We restate Theorem 3 as follows.

Theorem 6. *Under the above assumptions and notations, assume that the following condition holds:*

(A) For any projection Φ with $\mathrm{Im}\Phi_2 \neq \emptyset$, there exist $(X^{e_1}, Y^{e_1}), (X^{e_2}, Y^{e_2}) \in T_{ad}$ such that $P(g(Y^{e_1})|\Phi(X^{e_1})) \neq P(g(Y^{e_2})|\Phi(X^{e_2}))$.

Then, there exists $\lambda^* \in \mathbb{R}$ such that a minimizer $(\theta^\dagger, \theta^\dagger_{ad}, \Phi^\dagger)$ of the objective function

$$\min_{\theta,\theta_{ad},\Phi} \left\{ \mathcal{R}^{(X^*,Y^*)}(p_\theta \circ \Phi) + \lambda^* \cdot \sum_{(X^e,Y^e)\in T_{ad}} \|\nabla_{\hat{\theta}_{ad}=\theta_{ad}} \mathcal{R}^{(X^e,g(Y^e))}(p^{\mathcal{Z}|\mathcal{H}}_{\hat{\theta}_{ad}} \circ \Phi)\|^2 \right\} \tag{9}$$

is o.o.d. optimial, i.e.,

$$p_{\theta^\dagger} \circ \Phi^\dagger \in \operatorname*{argmin}_{p_\theta:\mathcal{X}\to\mathcal{P}_\mathcal{Y}} \mathcal{R}^{o.o.d.}(p_\theta),$$

where p_θ and $p^{\mathcal{Z}|\mathcal{H}}_{\theta_{ad}}$ in $\min_{\theta,\theta_{ad},\Phi}$ run all the p.d.f.s, and Φ runs all the variable selections. The gradient $\nabla_{\theta_{ad}}$ should be understood as the functional derivative on the space of p.d.f.

Before proving Theorem 6, we prepare one lemma, which asserts that, if $\mathrm{Im}\Phi_2 \neq \emptyset$, at least one domain in T_{ad} has non-trivial gradient:

Lemma 7.

$$\min_{\theta_{ad},\Phi:\mathrm{Im}\Phi_2\neq\emptyset} \sum_{(X^e,Y^e)\in T_{ad}} \|\nabla_{\hat{\theta}_{ad}=\theta_{ad}} \mathcal{R}^{(X^e,g(Y^e))}(p^{\mathcal{Z}|\mathcal{H}}_{\hat{\theta}_{ad}} \circ \Phi)\|^2 \ > \ 0.$$

Proof. It suffices to prove that, for any projection Φ with $\mathrm{Im}\Phi_2 \neq \emptyset$ and $p^{\mathcal{Z}|\mathcal{H}}_{\theta_{ad}}$, there is $(X^e, Y^e) \in T_{ad}$ such that $\|\nabla_{\hat{\theta}_{ad}=\theta_{ad}} \mathcal{R}^{(X^e,g(Y^e))}(p^{\mathcal{Z}|\mathcal{H}}_{\hat{\theta}_{ad}} \circ \Phi)\|^2 \neq 0$. We prove this by contradiction. Suppose that there exist a projection Φ with $\mathrm{Im}\Phi_2 \neq \emptyset$ and $p^{\mathcal{Z}|\mathcal{H}}_{\theta_{ad}}$ which satisfy

$$\|\nabla_{\hat{\theta}_{ad}=\theta_{ad}} \mathcal{R}^{(X^e,g(Y^e))}(p^{\mathcal{Z}|\mathcal{H}}_{\hat{\theta}_{ad}} \circ \Phi)\|^2 = 0 \quad (\forall (X^e, Y^e) \in T_{ad}).$$

From Assumption (A), take (X^{e_1}, Y^{e_1}) and (X^{e_2}, Y^{e_2}) in T_{ad} such that $P(g(Y^{e_1})|\Phi(X^{e_1})) \neq P(g(Y^{e_2})|\Phi(X^{e_2}))$.

Note that the risk is defined by the cross-entropy loss:

$$\mathcal{R}^{(X^e,g(Y^e))}(p^{\mathcal{Z}|\mathcal{H}}_{\hat{\theta}_{ad}} \circ \Phi) = -\int \log p^{\mathcal{Z}|\mathcal{H}}_{\hat{\theta}_{ad}}(g(Y^e)|\Phi(X^e)) dP_{X^e,Y^e}.$$

It is well known that this is minimized in the space of probability distributions if and only if $p^{\mathcal{Z}|\mathcal{H}}_{\hat{\theta}_{ad}}$ equals to $P(Y^e|\Phi(X^e))$. From $\|\nabla_{\hat{\theta}_{ad}=\theta_{ad}} \mathcal{R}^{(X^e,g(Y^e))}(p^{\mathcal{Z}|\mathcal{H}}_{\hat{\theta}_{ad}} \circ \Phi)\|^2 = 0$ for (X^{e_1}, Y^{e_1}) and (X^{e_2}, Y^{e_2}), we can conclude that $p^{\mathcal{Z}|\mathcal{H}}_{\theta_{ad}}$ should equal to both of $P(g(Y^{e_1})|\Phi(X^{e_1}))$ and $P(g(Y^{e_2})|\Phi(X^{e_2}))$. This contradicts with the assumption $P(g(Y^{e_1})|\Phi(X^{e_1})) \neq P(g(Y^{e_2})|\Phi(X^{e_2}))$. □

Proof of Theorem 6

Let Φ^{id} denote the identity map of $\mathcal{X}$. Define the constants C_1, C_2, and C_3 by

$$C_1 := \mathcal{R}^{(X^*,Y^*)}(p^{*,\Phi^{id}} \circ \Phi^{id}) = H(Y^*|X^*),$$
$$C_2 := \mathcal{R}^{(X^*,Y^*)}(p^{*,\Phi^I} \circ \Phi^I) = H(Y^*|X_1^*) = H(Y^I|X_1^I),$$
$$C_3 := \frac{C_2 - C_1}{\min_{\theta_{ad},\Phi:\mathrm{Im}\Phi_2\neq\emptyset} \sum_{(X^e,Y^e)\in T_{ad}} \|\nabla_{\hat{\theta}_{ad}=\theta_{ad}} \mathcal{R}^{(X^e,g(Y^e))}(p^{\mathcal{Z}|\mathcal{H}}_{\hat{\theta}_{ad}} \circ \Phi)\|^2},$$

where $H(Y^I|X_1^I)$ and $H(Y^*|X^*)$ denote the conditional entropy. Note that C_3 is well-defined because of the positivity result of Lemma 7.

Take λ^* such that $\lambda^* > C_3$. For notational simplicity, the objective function (9) is denoted by $O(\theta, \theta_{ad}, \Phi)$; namely,

$$O(\theta, \theta_{ad}, \Phi) := \mathcal{R}^{(X^*,Y^*)}(p_\theta \circ \Phi) + \lambda^* \cdot \sum_{(X^e,Y^e)\in T_{ad}} \|\nabla_{\hat{\theta}_{ad}=\theta_{ad}} \mathcal{R}^{(X^e,g(Y^e))}(p^{\mathcal{Z}|\mathcal{H}}_{\hat{\theta}_{ad}} \circ \Phi)\|^2.$$

We prove the theorem in three steps.

Step 1 $\min_{p:\mathcal{X}\to\mathcal{P}_\mathcal{Y}} \mathcal{R}^{o.o.d.}(p) = H(Y^I|X_1^I)$.

proof of Step 1
We will prove $p^I \in \underset{p:\mathcal{X}\to\mathcal{P}_\mathcal{Y}}{\operatorname{argmin}} \mathcal{R}^{o.o.d.}(p)$. From the definition

$$\mathcal{R}^{o.o.d.}(p) = \max_{(X^e,Y^e)\in T_{all}} -\int \log p(Y^e|X^e) dP_{Y^e,X^e},$$

$p^I \in \underset{p:\mathcal{X}\to\mathcal{P}_\mathcal{Y}}{\operatorname{argmin}} \mathcal{R}^{o.o.d.}(p)$ holds if and only if

$$\max_{(X^e,Y^e)\in T_{all}} -\int \log p_\theta(Y^e|X^e) dP_{Y^e,X^e} \geq \max_{(X^e,Y^e)\in T_{all}} -\int \log p^I(Y^e|X_1^e) dP_{Y^e,X^e}$$

for any $p_\theta : \mathcal{X} \to \mathcal{P}_\mathcal{Y}$. Note that, as discussed before Theorem 6, for any $(X^e, Y^e) \in T_{all}$, we have $P_{Y^e|X_1^e} = P_{Y^I|X_1^I}$. Then, it suffices to prove that for any p_θ there exists $(X^{e'}, Y^{e'}) \in T_{all}$ such that

$$\int -\log p_\theta(Y^{e'}|X^{e'}) dP_{Y^{e'},X^{e'}} \geq \int -\log p^I(Y^I|X_1^I) dP_{X^e,Y^e}. \tag{10}$$

Define $(X^{e'}, Y^{e'}) \in T_{all}$ such that its distribution is the direct product $P_{X_1^I,Y^I} \otimes P_{X_2^{e'}}$, where $P_{X_2^{e'}}$ is an arbitrary distribution on $\mathcal{X}_2$. In this case, the left hand side of (10) is given by

$$\begin{aligned}\int -\log p_\theta(Y^{e'}|X^{e'}) dP_{Y^{e'},X^{e'}} &= \int -\log p_\theta(Y^{e'}|X_1^{e'}, X_2^{e'}) dP_{Y^{e'},X^{e'}} \\ &= \int dP_{X_2^{e'}} \int -\log p_\theta(Y^I|X_1^I, X_2^{e'}) dP_{X_1^I,Y^I}.\end{aligned} \tag{11}$$

We can see that, for any $x_2 \in \mathcal{X}_2$, the inequality

$$\int -\log p_\theta(Y^I|X_1^I, X_2^{e'} = x_2)) dP_{X_1^I,Y^I} \geq \int -\log p^I(Y^I|X_1^I) dP_{X_1^I,Y^I}$$

holds, since the minimum of the cross entropy loss is attained at the conditional p.d.f. p^I. Integrating this inequality with $P_{X_2^{e'}}$, we have

$$\int dP_{X_2^e} \int -\log p_\theta(Y^I|X_1^I, X_2^e) dP_{X_1^I,Y^I} \geq \int -\log p^I(Y^I|X_1^I) dP_{X_1^I,Y^I}. \tag{12}$$

Eqs. (11) and (12) show (10), from which the assertion is obtained by $-\int \log p^I(Y^I|X_1^I) dP_{X_1^I,Y^I} = H(Y^I|X_1^I)$.

Step 2 Any minimizer of the objective function,

$$(\theta^\dagger, \theta^\dagger_{ad}, \Phi^\dagger) \in \underset{\theta,\theta_{ad},\Phi}{\operatorname{argmin}} O(\theta, \theta_{ad}, \Phi),$$

satisfies $\mathrm{Im}\Phi_2^\dagger = \emptyset$.

proof of Step 2

It suffices to prove that $\min_{\Phi:\mathrm{Im}\Phi_2=\emptyset,\theta,\theta_{ad}} O(\theta,\theta_{ad},\Phi) < \min_{\Phi:\mathrm{Im}\Phi_2\neq\emptyset,\theta,\theta_{ad}} O(\theta,\theta_{ad},\Phi)$. First, we have

$$
\begin{aligned}
&\min_{\Phi:\mathrm{Im}\Phi_2\neq\emptyset,\theta,\theta_{ad}} O(\theta,\theta_{ad},\Phi)\\
&= \min_{\Phi:\mathrm{Im}\Phi_2\neq\emptyset,\theta,\theta^{ad}} \left\{ \mathcal{R}^{(X^*,Y^*)}(p_\theta\circ\Phi) + \lambda^*\cdot \sum_{(X^e,Y^e)\in T_{ad}} \|\nabla_{\hat\theta_{ad}=\theta_{ad}} \mathcal{R}^{(X^e,g(Z^e))}(p^{\mathcal{Z}|\mathcal{H}}_{\hat\theta_{ad}}\circ\Phi)\|^2 \right\}.\\
&> \min_{\Phi:\mathrm{Im}\Phi_2\neq\emptyset,\theta,\theta_{ad}} \left\{ \mathcal{R}^{(X^*,Y^*)}(p_\theta\circ\Phi) + \frac{C_2-C_1}{\min_{\theta_{ad},\Phi:\mathrm{Im}\Phi_2\neq\emptyset}\sum_{(X^e,Y^e)\in T_{ad}} \|\nabla_{\hat\theta_{ad}=\theta_{ad}} \mathcal{R}^{(X^e,g(Y^e))}(p^{\mathcal{Z}|\mathcal{H}}_{\hat\theta_{ad}}\circ\Phi)\|^2} \right.\\
&\qquad\qquad \left. \times \sum_{(X^e,Y^e)\in T_{ad}} \|\nabla_{\hat\theta_{ad}=\theta_{ad}} \mathcal{R}^{(X^e,g(Y^e))}(p^{\mathcal{Z}|\mathcal{H}}_{\hat\theta_{ad}}\circ\Phi)\|^2 \right\}\\
&\geq \min_{\Phi:\mathrm{Im}\Phi_2\neq\emptyset,\theta,\theta_{ad}} \{\mathcal{R}^{(X^*,Y^*)}(p_\theta\circ\Phi) + C_2 - C_1\}\\
&= \min_{\Phi:\mathrm{Im}\Phi_2\neq\emptyset,\theta,\theta_{ad}} \{\mathcal{R}^{(X^*,Y^*)}(p_\theta\circ\Phi)\} + C_2 - C_1\\
&\geq \mathcal{R}^{(X^*,Y^*)}(p^{*,\Phi^{id}}\circ\Phi^{id}) + C_2 - C_1 = C_2.
\end{aligned}
$$

On the other hand, by taking $\Phi=\Phi^I$, we obtain

$$
\begin{aligned}
&\min_{\Phi:\mathrm{Im}\Phi_2=\emptyset,\theta,\theta_{ad}} O(\theta,,\theta_{ad},\Phi)\\
&\qquad\qquad \leq \mathcal{R}^{(X^*,Y^*)}(p^I) + \lambda^*\cdot \sum_{(X^e,Y^e)\in T_{ad}} \|\nabla_{\hat\theta_{ad}=\theta^*_{ad}} \mathcal{R}^{(X^e,g(Y^e))}(p^{\mathcal{Z}|\mathcal{H}}_{\hat\theta_{ad}}\circ\Phi^I)\|^2.
\end{aligned}
$$

Since $p^{\mathcal{Z}|\mathcal{H}}_{\hat\theta_{ad}}\circ\Phi^I = p^I(g(Y^I)|X^I_1)$ does not depend on θ_{ad}, the gradient is zero, and therefore

$$
\min_{\Phi:\mathrm{Im}\Phi_2=\emptyset,\theta,\theta_{ad}} O(\theta,,\theta_{ad},\Phi) \leq \mathcal{R}^{(X^*,Y^*)}(p^I) = C_2.
$$

We thus obtain

$$
\min_{\Phi:\mathrm{Im}\Phi_2=\emptyset,\theta,\theta_{ad}} O(\theta,\theta_{ad},\Phi) \leq C_2 < \min_{\Phi:\mathrm{Im}\Phi_2\neq\emptyset,\theta,\theta_{ad}} O(\theta,\theta_{ad},\Phi),
$$

which completes the proof.

Step 3 If $(p_{\theta^\dagger}, p^{\mathcal{Z}|\mathcal{H}}_{\theta^\dagger_{ad}}, \Phi^\dagger) \in \operatorname*{argmin}_{\theta,\theta_{ad},\Phi} O(\theta,\theta^{ad},\Phi)$, then $\mathcal{R}^{o.o.d.}(p_{\theta^\dagger}\circ\Phi^\dagger) = H(Y^I|X^I_1)$.

proof of Step 3

From Step 1, we have $H(Y^I|X^I_1) \leq \mathcal{R}^{o.o.d.}(p_{\theta^\dagger}\circ\Phi^\dagger)$. We will probe the converse inequality.

From Step 2, we have $\mathrm{Im}\Phi^\dagger_2=\emptyset$. This tells $\mathcal{R}^{o.o.d.}(p_{\theta^\dagger}\circ\Phi^\dagger) = \mathcal{R}^{e^*}(p_{\theta^\dagger}\circ\Phi^\dagger)$, since $P_{X_1,Y}$ are the same for all elements in T_{all}. Therefore,

$$
\begin{aligned}
&\mathcal{R}^{o.o.d.}(p_{\theta^\dagger}\circ\Phi^\dagger) = \mathcal{R}^{(X^*,Y^*)}(p_{\theta^\dagger}\circ\Phi^\dagger)\\
&\leq \min_{\theta_{ad}} \left\{ \mathcal{R}^{(X^*,Y^*)}(p_{\theta^\dagger}\circ\Phi^\dagger) + \lambda^*\cdot \sum_{(X^e,Y^e)\in T_{ad}} \|\nabla_{\hat\theta_{ad}=\theta^*_{ad}} \mathcal{R}^{(X^e,g(Y^e))}(p^{\mathcal{Z}|\mathcal{H}}_{\hat\theta_{ad}}\circ\Phi)\|^2 \right\}\\
&= \min_{\Phi,\theta,\theta_{ad}} \left\{ \mathcal{R}^{(X^*,Y^*)}(p_\theta\circ\Phi) + \lambda^*\cdot \sum_{(X^e,Y^e)\in T_{ad}} \|\nabla_{\hat\theta_{ad}=\theta_{ad}} \mathcal{R}^{(X^e,g(Y^e))}(p^{\mathcal{Z}|\mathcal{H}}_{\hat\theta_{ad}}\circ\Phi)\|^2 \right\}\\
&\leq C_2 = H(Y^I|X^I_1).
\end{aligned}
$$

Final step for the proof of Theorem 6

For $(\theta^\dagger,\theta^\dagger_{ad},\Phi^\dagger) \in \operatorname*{argmin}_{\theta,\theta_{ad},\Phi} O(\theta,\theta_{ad},\Phi)$, Step 1 and Step 3 show

$$
\mathcal{R}^{o.o.d.}(p_{\theta^\dagger}\circ\Phi^\dagger) = H(Y^I|X^I_1) = \min_{p:\theta\to\mathcal{P}_{\mathcal{Y}}} \mathcal{R}^{o.o.d.}(p),
$$

which completes the proof.

C Proof of Theorem 4

Before the proof, let us rearrange some notations introduced in Section 4.2. Notations are the same as in Appendix B. Recall that we assume, given hyperparameter λ, the minimization of (5) achieves the global optimum perfectly, which yields the projection (variable selection) $\Phi^\lambda(x) : \mathcal{X} \to \mathbb{R}^{n_\lambda}$ ($n_\lambda \leq n_1 + n_2$) and the conditional p.d.f. of $P_{Y^{e^*}|\Phi^\lambda(X^{e^*})}$, denoted by $p^{*,\lambda}(y|\Phi^\lambda(x))$. The $\mathcal{X}_1$ and $\mathcal{X}_2$ components of $\Phi^\lambda(X)$ are denoted by $\Phi_1^\lambda(X)$ and $\Phi_2^\lambda(X)$, respectively.

For $\lambda \in \Lambda$ and the training variable (X^*, Y^*) for the target task, the conditional p.d.f. of $P(Y^*|\Phi^\lambda(X^*))$ given the selected variables is denoted by $p^{*,\lambda} : \mathbb{R}^{n_\lambda} \to \mathcal{P}_\mathcal{Y}$. Define $\mathcal{R}^{o.o.d.}(\lambda)$ and $\mathcal{R}^I(\lambda)$ by

$$\mathcal{R}^{o.o.d.}(\lambda) := \max_{(X,Y)\in T_{all}} \mathcal{R}^{(X,Y)}(p^{*,\lambda} \circ \Phi^\lambda),$$

$$\mathcal{R}^I(\lambda) := \max\left\{ \max_{(X,Y)\in T_{ad}} \mathcal{R}^{(X,g(Y))}(p^{*,\lambda} \circ \Phi^\lambda), \mathcal{R}^{(X^*,Y^*)}(p^{*,\lambda} \circ \Phi^\lambda) \right\},$$

respectively. We restate Theorem 4 with some notation arrangements:

Theorem 8. *Under the above notations, assume the following two conditions:*

(I) there is $\lambda^I \in \Lambda$ such that $\Phi^{\lambda^I} = \Phi^{\mathcal{X}_1}$, where $\Phi^{\mathcal{X}_1}$ is the projection to the $\mathcal{X}_1$-components.

(II) Let p^* be the p.d.f of $P_{X^*,g(Y^*)}$. For any λ with $\mathrm{Im}\Phi_2^\lambda \neq \emptyset$, there is $(X^{e_\lambda}, Y^{e_\lambda}) \in T_{ad}$ such that

$$(x, z) \sim P_{X^{e_\lambda},g(Y^{e_\lambda})} \text{ satisfies } p^*(z|\Phi^\lambda(x)) \leq e^{-\beta} - \varepsilon \text{ with probability } 1 \text{ in } P_{X^{e_\lambda},g(Y^{e_\lambda})}.$$

Here, $\varepsilon \in \mathbb{R}_{>0}$ is a sufficiently small positive real number (that is, $0 < \varepsilon \ll 1$) and $\beta := H(Y^*|(X_1^*))$ is the conditional entropy of $((X_1^*), Y^*)$. Then, we have

$$\operatorname*{argmin}_{\lambda\in\Lambda} \mathcal{R}^I(\lambda) \subset \operatorname*{argmin}_{\lambda\in\Lambda} \mathcal{R}^{o.o.d.}(\lambda).$$

To prove Theorem 8, we prepare three lemmas, in which the notations are the same as in Theorem 8 and conditions (I) and (II) in Theorem 8 are also imposed.

Lemma 9. $\lambda^I \in \operatorname*{argmin}_{\lambda\in\Lambda} \mathcal{R}^{o.o.d.}(\lambda)$.

Lemma 10. *If $\hat{\lambda} \in \operatorname*{argmin}_{\lambda\in\Lambda} \mathcal{R}^I(\lambda)$, then $\mathrm{Im}\Phi_2^{\hat{\lambda}} = \emptyset$.*

Lemma 11. *If $\hat{\lambda} \in \Lambda$ satisfies $\mathrm{Im}\Phi_2^{\hat{\lambda}} = \emptyset$, then $\mathcal{R}^I(\hat{\lambda}) = \mathcal{R}^{o.o.d.}(\hat{\lambda})$.*

we prove Theorem 8 based on the above lemmas, before proving them.

proof of Theorem 8.
Take $\hat{\lambda} \in \operatorname{argmin} \mathcal{R}^I(\lambda)$. Then, $\mathrm{Im}\Phi_2^{\hat{\lambda}} = \emptyset$ holds by Lemma 10 and therefore, $\mathcal{R}^I(\hat{\lambda}) = \mathcal{R}^{o.o.d.}(\hat{\lambda})$ holds by Lemma 11. Moreover, $\mathcal{R}^{o.o.d.}(\hat{\lambda}) \geq \mathcal{R}^{o.o.d.}(\lambda^I)$ holds by Lemma 9 and $\mathcal{R}^{o.o.d.}(\lambda^I) = \mathcal{R}^I(\lambda^I)$ holds by Lemma 11 (since Φ^{λ^I} is the projection onto $\mathcal{X}_1$, $\mathrm{Im}\Phi_2^{\lambda^I} = \emptyset$). By the assumption $\hat{\lambda} \in \operatorname*{argmin}_{\lambda\in\Lambda} \mathcal{R}^I(\lambda)$, $\mathcal{R}^I(\lambda^I) \geq \mathcal{R}^I(\hat{\lambda})$ holds. Arranging these inequalities, we obtain

$$\mathcal{R}^I(\hat{\lambda}) = \mathcal{R}^{o.o.d.}(\hat{\lambda}) \geq \mathcal{R}^{o.o.d.}(\lambda^I) = \mathcal{R}^I(\lambda^I) \geq \mathcal{R}^I(\hat{\lambda}), \tag{13}$$

in which the inequalities must be equalities. Hence, we obtain $\mathcal{R}^{o.o.d.}(\hat{\lambda}) = \mathcal{R}^{o.o.d.}(\lambda^I)$. Because λ^I achieves the minimum of $\mathcal{R}^{o.o.d.}$ (Lemma 9), so does $\hat{\lambda}$, which concludes the proof. □

Since Lemma 9 is proven in the proof of Theorem 6 (especially, the proof in Step 1), we may prove the others.

proof of Lemma 10.
Let us prove the contraposition of Lemma 10. Take $\hat{\lambda} \in \Lambda$ with $\mathrm{Im}\Phi_2^{\hat{\lambda}} \neq \emptyset$. To prove that $\hat{\lambda} \notin \operatorname{argmin} \mathcal{R}^I(\lambda)$, we may prove that $\mathcal{R}^I(\hat{\lambda}) > \mathcal{R}^I(\lambda^I)$ since $\lambda^I \in \Lambda$ (Assumption (I) in the statement). It then suffices to prove the following:

$$\text{there exists } (\bar{X}, \bar{Y}) \in T_{ad} \text{ such that } \int -\log p^{*,\hat{\lambda}}(g(\bar{Y})|\Phi^{\hat{\lambda}}(\bar{X}))dP_{\bar{X},g(\bar{Y})} > \mathcal{R}^I(\lambda^I). \tag{14}$$

From Condition (II), we can take $(X^{e_{\hat{\lambda}}}, Y^{e_{\hat{\lambda}}}) \in T_{ad}$ such that

$$(x, z) \sim P_{X^{e_{\hat{\lambda}}}, g(Y^{e_{\hat{\lambda}}})} \text{ satisfies } p^*(z|\Phi^{\hat{\lambda}}(x)) \leq e^{-\beta} - \varepsilon \text{ with probability } 1.$$

To prove (14), we prepare one supplementary inequality:

Supplementary Inequality

$$\int -\log p^{*,\hat{\lambda}}\big(g(Y^{e_{\hat{\lambda}}})|\Phi^{\hat{\lambda}}(X^{e_{\hat{\lambda}}})\big) dP_{X^{e_{\hat{\lambda}}}, g(Y^{e_{\hat{\lambda}}})} \geq -\log\left\{e^{-\beta} - \epsilon\right\}.$$

This inequality can be easily seen; from the way of taking $e_{\hat{\lambda}}$, we have

$$-\log p^*(z|\Phi^{\hat{\lambda}}(x)) \geq -\log\{e^{-\beta} - \varepsilon\}$$

with probability 1 with respect to $(x, z) \sim P_{X^{e_{\hat{\lambda}}}, g(Y^{e_{\hat{\lambda}}})}$, and thus the integration proves the inequality.

Proof of Inequality (14).
It follows from the above supplementary inequality that

$$\int -\log p^{*,\hat{\lambda}}(g(Y^{e_{\hat{\lambda}}})|\Phi^{\hat{\lambda}}(X^{e_{\hat{\lambda}}})) dP_{X^{e_{\hat{\lambda}}}, g(Y^{e_{\hat{\lambda}}})} \geq -\log\left\{e^{-\beta} - \epsilon\right\} > \beta = H(Y^*|X_1^*). \tag{15}$$

Since $\Phi^{\lambda^I} = \Phi^{\mathcal{X}_1}$ by Condition (I), the discussion at (8) tells that $\mathcal{R}^I(\lambda^I) = H(Y^I|X_1^I) = H(Y^*|X_1^*)$, which concludes (14) and the proof.

Proof of Lemma 11.
Take $\hat{\lambda} \in \Lambda$ that satisfies $\mathrm{Im}\Phi_2^{\hat{\lambda}} = \emptyset$. Then, $P_{\Phi^{\hat{\lambda}}(X),Y} = P_{\Phi^{\hat{\lambda}}(X^I),Y^I}$ holds for any $(X, Y) \in T_{all}$ because of $P_{X_1,Y} = P_{X_1^I,Y}$, and therefore, $\mathcal{R}^{(X,g(Y))}(p^{*,\hat{\lambda}} \circ \Phi^{\hat{\lambda}}) = \mathcal{R}^{(X^I,g(Y^I))}(p^{*,\hat{\lambda}} \circ \Phi^{\hat{\lambda}})$ and $\mathcal{R}^{(X^*,Y^*)}(p^{*,\hat{\lambda}} \circ \Phi^{\hat{\lambda}}) = \mathcal{R}^{(X^I,Y^I)}(p^{*,\hat{\lambda}} \circ \Phi^{\hat{\lambda}})$ hold. These two equalities lead the following equality:

$$\begin{aligned}\mathcal{R}^I(\hat{\lambda}) &= \max\left\{\max_{(X,Y)\in T_{ad}} \mathcal{R}^{(X,g(Y))}(p^{*,\hat{\lambda}} \circ \Phi^{\hat{\lambda}}), \mathcal{R}^{(X^*,Y^*)}(p^{*,\hat{\lambda}} \circ \Phi^{\hat{\lambda}})\right\} \\ &= \max\left\{\mathcal{R}^{(X^I,g(Y^I))}(p^{*,\hat{\lambda}} \circ \Phi^{\hat{\lambda}}), \mathcal{R}^{(X^I,Y^I)}(p^{*,\hat{\lambda}} \circ \Phi^{\hat{\lambda}})\right\} \end{aligned} \tag{16}$$

It follows from Theorem 2 that

$$\begin{aligned}&R^{(X^I,Y^I)}(p^{*,\hat{\lambda}} \circ \Phi^{\hat{\lambda}}) \\ &= \mathcal{R}^{(X^I,g(Y^I))}(p^{*,\hat{\lambda}} \circ \Phi^{\hat{\lambda}}) \\ &\quad + \sum_{z^{\cancel{*}} \in \mathcal{Z}^{\cancel{*}}} P(Y^I = g^{-1}(z^{\cancel{*}})) \int -\log p^{*,\hat{\lambda}}(Y^I|\Phi^{\hat{\lambda}}(X^I), g(Y^I) = z^{\cancel{*}}) dP_{X^I,Y^I|g(Y^I)=z^{\cancel{*}}} \\ &\geq \mathcal{R}^{(X^I,g(Y^I))}(p^{*,\hat{\lambda}} \circ \Phi^{\hat{\lambda}})\end{aligned}$$

Therefore, from (16), we have $\mathcal{R}^I(\hat{\lambda}) = \mathcal{R}^{(X^I,Y^I)}(p^{*,\hat{\lambda}} \circ \Phi^{\hat{\lambda}})$. Since $P_{\Phi^{\hat{\lambda}}(X),Y}$ are the same for any elements in T_{all}, we obtain

$$\mathcal{R}^{(X^I,Y^I)}(p^{*,\hat{\lambda}} \circ \Phi^{\hat{\lambda}}) = \max_{(X,Y)\in T_{all}} \mathcal{R}^{(X,Y)}(p^{*,\hat{\lambda}} \circ \Phi^{\hat{\lambda}}) = \mathcal{R}^{o.o.d.}(p^{*,\hat{\lambda}} \circ \Phi^{\hat{\lambda}}),$$

which concludes the proof.

D Proof of Theorem 5

We restate Theorem 5 with some notation arrangements:

Theorem 12. *Notations are the same as in the statement of Theorem 8. Define $\mathcal{R}^{II}(\lambda)$ by*

$$\mathcal{R}^{II}(\lambda) := \max_{(X,Y)\in T_{ad}\cup\{(X^*,Y^*)\}} \left\{\mathcal{R}^{(X,g(Y))}(p^{*,\lambda} \circ \Phi^{\lambda}) + D_\lambda(Y)\right\},$$

where the correction term $D_\lambda(Y)$ is defined by

$$D_\lambda(Y) := \sum_{z^{\cancel{*}} \in \mathcal{Z}^{\cancel{*}}} \left\{P(g(Y) = z^{\cancel{*}}) \int -\log p^{*,\lambda}(Y^*|\Phi^{\lambda}(X^*), g(Y^*) = z^{\cancel{*}}) dP_{(X^*,Y^*)|g(Y^*)=z^{\cancel{*}}}\right\}$$

In addition to the condition (I), assume the following condition (II)':

(II)' Let p^* be the p.d.f. of $P_{X^*,g(Y^*)}$. For any λ with $\mathrm{Im}\Phi_2^\lambda \neq \emptyset$, there is $(X^{e_\lambda}, Y^{e_\lambda}) \in T_{ad}$ such that $(x,z) \sim P_{X^{e_\lambda},g(Y^{e_\lambda})}$ satisfies $p^*(z|\Phi^\lambda(x)) \leq e^{-\beta_\lambda} - \varepsilon$ with probability 1 in $P_{X^{e_\lambda},g(Y^{e_\lambda})}$.

Here, ε is some positive real number and

$$\beta_\lambda := H(Y^*|X_1^*) - D_\lambda(Y^*).$$

Then, we have

$$\operatorname*{argmin}_{\lambda\in\Lambda} \mathcal{R}^{II}(\lambda) \subset \operatorname*{argmin}_{\lambda\in\Lambda} \mathcal{R}^{o.o.d.}(\lambda).$$

Note that, in $D_\lambda(Y)$, although the random variable Y is given by $(X,Y) \in T_{all}$, the marginal distributions of Ys are the same by the assumption of T_{all}. Thus, hereafter, we use D_λ for the notation, and

$$D_\lambda = \sum_{z^{\cancel{*}} \in \mathcal{Z}^{\cancel{*}}} \left\{ P(g(Y^*) = z^{\cancel{*}}) \int -\log p^{*,\lambda}(Y^*|\Phi^\lambda(X^*), g(Y^*) = z^{\cancel{*}}) dP_{(X^*,Y^*)|g(Y^*)=z^{\cancel{*}}} \right\}.$$

Note also that $\beta_\lambda = H(Y^*|X_1^*) - D_\lambda$. We first show lemmas before the proof of the theorem.

Lemma 13. *If $\hat\lambda \in \operatorname*{argmin}_{\lambda\in\Lambda} \mathcal{R}^{II}(\lambda)$, then $\mathrm{Im}\Phi_2^{\hat\lambda} = \emptyset$.*

Lemma 14. *If $\hat\lambda \in \Lambda$ satisfies $\mathrm{Im}\Phi_2^{\hat\lambda} = \emptyset$, then $\mathcal{R}^{II}(\hat\lambda) = \mathcal{R}^{o.o.d.}(\hat\lambda)$.*

proof of Theorem 12
Combining the above two lemmas and Lemma 9, we can derive the required assertion in essentially the same manner as in the proof of Theorem 8.

proof of Lemma 13.
Let us prove the contraposition of Lemma 13. Take $\hat\lambda \in \Lambda$ with $\mathrm{Im}\Phi_2^{\hat\lambda} \neq \emptyset$. To prove that $\hat\lambda \notin \operatorname{argmin} \mathcal{R}^{II}(\lambda)$, we may prove that $\mathcal{R}^{II}(\hat\lambda) > \mathcal{R}^{II}(\lambda^I)$ since $\lambda^I \in \Lambda$ (Assumption (I) in the statement). To show this, it suffices to prove the following statement:

$$\text{there is } (\bar X, \bar Y) \in T_{ad} \text{ such that } \mathcal{R}^{(\bar X, g(\bar Y))}(\hat\lambda) + D_{\hat\lambda} > \mathcal{R}^{II}(\lambda^I). \tag{17}$$

Take $(X^{e_{\hat\lambda}}, Y^{e_{\hat\lambda}}) \in T_{ad}$ as in Condition (II)'. Then, in the same way as the proof of Lemma 10, we have the following inequality:

$$\int -\log p^{*,\hat\lambda}\big(g(Y^{e_{\hat\lambda}})|\Phi^{\hat\lambda}(X^{e_{\hat\lambda}})\big) dP_{X^{e_{\hat\lambda}},g(Y^{e_{\hat\lambda}})} \geq -\log\left\{e^{-\beta_{\hat\lambda}} - \epsilon\right\},$$

which leads us to obtain

$$\mathcal{R}^{(X^{e_{\hat\lambda}}, g(Y^{e_{\hat\lambda}}))}(\hat\lambda) + D_{\hat\lambda} > \beta_{\hat\lambda} + D_{\hat\lambda} = H(Y^*|X_1^*) = \mathcal{R}^{(Y^*,X^*)}(p^{*,\lambda^I} \circ \Phi^{\lambda^I}). \tag{18}$$

On the other hand, for any $(X,Y) \in T_{all}$ the marginal distribution of $(Y, \Phi^I(X))$ is the same as that of (Y^*, X_1^*). Noting that $\mathcal{R}^{(X,g(Y))}(p^{*,\lambda^I} \circ \Phi^{\lambda^I}) + D_{\lambda^I}$ depends only on (Y, X_1), we have

$$\mathcal{R}^{II}(\lambda^I) = \mathcal{R}^{(X^*,g(Y^*))}(p^{*,\lambda^I} \circ \Phi^{\lambda^I}) + D_{\lambda^I}. \tag{19}$$

Now, Lemma 2 implies

$$\mathcal{R}^{(Y^*,X^*)}(p^{*,\lambda^I} \circ \Phi^{\lambda^I}) = \mathcal{R}^{(X^*,g(Y^*))}(p^{*,\lambda^I} \circ \Phi^{\lambda^I}) + D_{\lambda^I}. \tag{20}$$

From (18), (19), and (20), we thus have

$$\mathcal{R}^{(X^{e_{\hat\lambda}}, g(Y^{e_{\hat\lambda}}))}(p^{*,\lambda^I} \circ \Phi^{\lambda^I}) + D_{\hat\lambda} > \mathcal{R}^{II}(\lambda^I),$$

which shows (17) and completes the proof.

proof of Lemma 14.
Take $\hat\lambda \in \Lambda$ such that $\mathrm{Im}\Phi_2^{\hat\lambda} = \emptyset$. It follows from $\mathrm{Im}\Phi_2^{\hat\lambda} = \emptyset$ that $P_{\Phi^{\hat\lambda}(X),Y} = P_{\Phi^{\hat\lambda}(X^*),Y^*}$ holds for all $(X,Y) \in T_{all}$. Therefore,

$$\mathcal{R}^{o.o.d.}(\hat\lambda) = \max_{(X,Y)\in T_{all}} \mathcal{R}^{(X,Y)}(p^{*,\hat\lambda} \circ \Phi^{\hat\lambda}) = \mathcal{R}^{(X^*,Y^*)}(p^{*,\hat\lambda} \circ \Phi^{\hat\lambda}).$$

Likewise, from the condition of $\hat\lambda$, the definition of $\mathcal{R}^{II}(\hat\lambda)$ involves the same distribution for $(Y, \Phi^{\hat\lambda}(X))$, and thus

$$\mathcal{R}^{II}(\hat\lambda) = \mathcal{R}^{(X^*,g(Y^*))}(p^{*,\hat\lambda} \circ \Phi^{\hat\lambda}) + D_{\hat\lambda}.$$

In a similar way to the proof of Lemma 13, Theorem 2 tells

$$\mathcal{R}^{(X^*,Y^*)}(p^{*,\hat\lambda} \circ \Phi^{\hat\lambda}) = \mathcal{R}^{(X^*,g(Y^*))}(p^{*,\hat\lambda} \circ \Phi^{\hat\lambda}) + D_{\hat\lambda}.$$

This completes the proof.

E Sufficient Conditions of (ii) and (ii)'

In the section, we reveal sufficient conditions of e^* for there to exist $(X^{e_\lambda}, Y^{e_\lambda})$ that satisfies (ii) and (ii)' in Theorems 4 and 5, respectively.

Theorem 15. *Notations are the same as in Theorem 8. Assume that (X^*, Y^*) satisfies the following condition:*

(A2) For a sufficiently small $\varepsilon \ll 1$, any λ with $\mathrm{Im}\Phi_2^\lambda \neq \emptyset$, any $a \in \mathrm{Im}\Phi_1^\lambda$, and any $b \in \mathcal{Y}$, there exists $c(\lambda, a, b)$[2] such that

$$P(Y^* = b | \Phi_1^\lambda(X^*) = a, \Phi_2^\lambda(X^*) = c) \geq (1 - e^{-\beta}) + \varepsilon.$$

Then, for any λ with $\mathrm{Im}\Phi_2^\lambda \neq \emptyset$, there exists $(X^{e_\lambda}, Y^{e_\lambda}) \in T_{all}$ such that the inequality in Theorem 8 (ii) holds.

Remark. The condition (A2) means that, in the domain $e = e^*$, the affection of domain-specific factors ($= \mathcal{X}_2$) to the response variable Y^{e^*} is large; indeed, the inequality in (A2) means that, if λ fails to remove domain-specific factors ($i.e.$, $\mathrm{Im}\Phi_2^\lambda \neq \emptyset$), we can control the probability of $Y^{e^*} = b$ by selecting c for any $b \in \mathcal{Y}$. Note also that the inequality (A2) is a lower bound of the likelihood, while the condition in (ii), Theorem 8, is an upper bound of the likelihood. Although imposing an upper bound might look reasonable to reflect non-fitting of the projection Φ^λ, Theorem 15 shows that we can use lower bound as a sufficient condition.

Proof. Fix λ with $\mathrm{Im}\Phi_2^\lambda \neq \emptyset$. Take $(\bar{X}, \bar{Y}) \in T_{all}$ such that its probability measure corresponds to $\bar{P}_{X_2|Y,X_1} \times P_{Y^I, X_1^I}$, where $\bar{P}_{X_2|Y,X_1}$ is defined by, setting $\hat{c}(\hat{\lambda}, a, b)$ by

$$\hat{c}(\hat{\lambda}, a, b) \in \operatorname*{argmin}_{c \in \mathcal{X}_2} P(g(Y^*) = g(b) | \Phi_1^{\hat{\lambda}}(X^*) = \Phi_1^{\hat{\lambda}}(a), \Phi_2^{\hat{\lambda}}(X^*) = \Phi_2^{\hat{\lambda}}(c)),$$

$\bar{P}_{X_2|Y=b,X_1=a} := \delta_{X_2 = \hat{c}(\hat{\lambda}, a, b)}$. Here, for $c \in \mathcal{X}_2$, the probability measure $\delta_{X_2=c}$ on $\mathcal{X}_2$ denotes a Dirac measure at $c \in \mathcal{X}_2$.

Before proving Theorem 15, we prepare the following inequalities:
Supplementary Inequality 1.

$$\forall a \in \mathcal{X}_1, \forall b \in \mathcal{Y}, P\left(g(Y^*) = g(b) \,\middle|\, \Phi_1^{\hat{\lambda}}(X^*) = \Phi_1^{\hat{\lambda}}(a), \Phi_2^{\hat{\lambda}}(X^*) = \Phi_2^{\hat{\lambda}}\big(\hat{c}(\hat{\lambda}, a, b)\big)\right) \leq e^{-\beta} - \epsilon.$$

To see the fact, take $b^* \in \mathcal{Y}$ such that $g(b^*) \neq g(b)$[3]. Then, by the condition (ii) of Theorem 5 and $\mathrm{Im}\Phi_2^{\hat{\lambda}} \neq \emptyset$, there exists $c(\hat{\lambda}, a, b) \in \mathcal{X}_2$ such that

$$P\left(Y^* = b^* \,\middle|\, \Phi_1^{\hat{\lambda}}(X^*) = \Phi_1^{\hat{\lambda}}(a), \Phi_2^{\hat{\lambda}}(X^*) = \Phi_2^{\hat{\lambda}}\big(c(\hat{\lambda}, a, b)\big)\right) \geq 1 - e^{-\beta} + \epsilon.$$

Therefore,

$$\begin{aligned}
&P\left(g(Y^*) = g(b) \,\middle|\, \Phi_1^{\hat{\lambda}}(X^*) = \Phi_1^{\hat{\lambda}}(a), \Phi_2^{\hat{\lambda}}(X^*) = \Phi_2^{\hat{\lambda}}\big(\hat{c}(\hat{\lambda}, a, b)\big)\right) \\
&= \min_{c \in \mathcal{X}_2} P\big(g(Y^*) = g(b) | \Phi_1^{\hat{\lambda}}(X^*) = \Phi_1^{\hat{\lambda}}(a), \Phi_2^{\hat{\lambda}}(X^*) = \Phi_2^{\hat{\lambda}}(c)\big) \\
&\leq P\left(g(Y^*) = g(b) \,\middle|\, \Phi_1^{\hat{\lambda}}(X^*) = \Phi_1^{\hat{\lambda}}(a), \Phi_2^{\hat{\lambda}}(X^*) = \Phi_2^{\hat{\lambda}}\big(c(\hat{\lambda}, a, b)\big)\right) \\
&= 1 - \sum_{\bar{z} \neq g(b)} P\left(g(Y^*) = \bar{z} \,\middle|\, \Phi_1^{\hat{\lambda}}(X^*) = \Phi_1^{\hat{\lambda}}(a), \Phi_2^{\hat{\lambda}}(X^*) = \Phi_2^{\hat{\lambda}}\big(c(\hat{\lambda}, a, b)\big)\right) \\
&\leq 1 - P\left(g(Y^*) = g(b^*) \,\middle|\, \Phi_1^{\hat{\lambda}}(X^*) = \Phi_1^{\hat{\lambda}}(a), \Phi_2^{\hat{\lambda}}(X^*) = \Phi_2^{\hat{\lambda}}\big(c(\hat{\lambda}, a, b)\big)\right) \\
&\leq 1 - P\left(Y^* = b^* \,\middle|\, \Phi_1^{\hat{\lambda}}(X^*) = \Phi_1^{\hat{\lambda}}(a), \Phi_2^{\hat{\lambda}}(X^*) = \Phi_2^{\hat{\lambda}}\big(c(\hat{\lambda}, a, b)\big)\right) \\
&\leq 1 - (1 - e^{-\beta} + \epsilon) \\
&\leq e^{-\beta} - \epsilon.
\end{aligned}$$

[2] $c(\lambda, a, b)$ means $c \in \mathcal{X}_2$ is determined by given $\lambda \in \Lambda$, $a \in \mathcal{X}_1$, $b \in \mathcal{Y}$.

[3] Such b^* always exists by the following reason if $|\mathcal{Z}| \geq 2$ by the following reason. Take $\mathcal{Z} \ni z^* \neq g(b)$. By the surjectivity of g, $g^{-1}(z^*) \neq \emptyset$. Taking $b^* \in g^{-1}(z^*)$, $g(b^*) = z^* \neq g(b)$.

Proof of Theorem 15
We may prove that $P_{\bar{X},\bar{Y}}(A) = 1$ where

$$\left\{(x,y) \in \mathcal{X} \times \mathcal{Y} \middle| P\left(g(Y^*) = g(b) \middle| \Phi^{\hat{\lambda}}(X^*) = \Phi^{\hat{\lambda}}(x)\right) \leq e^{-\beta} - \epsilon \right\}.$$

Then,

$$\begin{aligned} P_{\bar{X},\bar{Y}}(A) &= \int 1_A dP_{\bar{X},\bar{Y}} = \int 1_A d(\bar{P}_{X_2|Y,X_1} \times P_{Y^I,X_1^I}) \\ &= \int dP_{Y^I,X_1^I} \int 1_A d\bar{P}_{X_2|Y,X_1} = \int dP_{Y^I,X_1^I}(x_1,y)\delta_{X_2=\hat{c}(\hat{\lambda},x_1,y)}(A_{(x_1,y)}) \end{aligned}$$

holds where $A_{(x_1,y)} := \{x_2 \in \mathcal{X}_2 | ((x_1,x_2),y) \in \mathcal{X} \times \mathcal{Y}\}$. By the Supplementary Inequality 1, $\hat{c}(\hat{\lambda},x_1,y) \in A_{(x_1,y)}$ holds and therefore, $\delta_{X_2=\hat{c}(\hat{\lambda},x_1,y)}(A_{(x_1,y)}) = 1$, which leads us to the equation $\int dP_{Y^I,X_1^I}(x_1,y)\delta_{X_2=\hat{c}(\hat{\lambda},x_1,y)}(A_{(x_1,y)}) = 1$.

□

Theorem 16. *Notations are same as in Theorem 8 and 12.* (X^*, Y^*) *satisfies the following condition:*

(A2)' For a sufficiently small $\varepsilon \ll 1$*, the following statement holds:*
$\forall \lambda$ *with* $\mathrm{Im}\Phi_2^\lambda \neq \emptyset$, $\forall \alpha \in \mathrm{Im}\Phi_1^\lambda$, $\forall b \in \mathcal{Y}$, $\exists c(\lambda,a,b)$ *s.t.* $P(Y^* = b|\Phi_1^\lambda(X^*) = a, \Phi_2^\lambda(X^*) = c) \geq (1 - e^{-\beta_\lambda}) + \varepsilon$.

Then, $\forall \lambda$ *with* $\mathrm{Im}\Phi_2^\lambda \neq \emptyset$*, there exists* $(X^{e_\lambda}, Y^{e_\lambda}) \in T_{all}$ *such that the inequality in (ii)' holds.*

The proof of Theorem 16 is essentially same as the one of Theorem 15 and therefore, we omit.

F The real-world feasibility of (ii) and (ii)'

In the subsection, we discuss the feasibility of (ii) and (ii)', and show these conditions are not necessarily strong.

First, we discuss the Condition (ii). Since $\beta = H(Y^e|\Phi^{\mathcal{X}_1}(X^e))$ is the conditional entropy, we have

$$0 \leq \beta \leq \frac{1}{|\mathcal{Y}|}$$

and hence

$$e^{-\frac{1}{|\mathcal{Y}|}} - \varepsilon \leq e^{-\beta} - \varepsilon \leq 1 - \varepsilon$$

holds. We can see that Condition (ii) is weak if $e^{-\beta} - \varepsilon$ approaches 1, or if β is small. Recall that $\Phi^{\mathcal{X}_1}(X^e)$ is the bias-removed feature of X^e (digit of CMNIST, or object of ImageNet, for example). We can then expect that, in many real-world settings, $\beta = H(Y^e|\Phi^{\mathcal{X}_1}(X^e))$ is often small, since the bias-removed feature $\Phi^{\mathcal{X}_1}(X^e)$ should have a large amount of information on the labels. Condition (ii) is satisfied if the likelihood $p^{e^*}(z|\Phi^\lambda(x))$ evaluated at a random point $(x,z) \sim P_{X^e,g(Y^e)}$ is bounded by the large value $e^{-\beta} - \varepsilon$ for at least one $e \in \mathcal{E}_{ad}$, so that the inequality in (ii) is likely to hold. Noting that (ii)' is weaker than (ii) (line 228 in the mainbody), the feasibility of (ii)' is concluded from one of (ii).

G Additional related works

Distributionally robust optimization The propose work tries to minimize the worst risk among risks on distributions perturbated from a training distribution [59–61]. The perturbated distributions are formalized as a small ε-ball centered at the training distribution evaluated by some divergence. In our setting, the change of distributions in training and testing is necessarily small; if the background changes drastically, it is expected that its corresponding distribution also changes drastically.

Concerning other strategies, [62] tries to obtain a de-biased feature Φ following the independence $\Phi(X) \perp\!\!\!\perp E$, seeing $\mathcal{E}$ as a random variable E. Recently, [63] consider the setting where there exists some f in the model that $f \neq f^{o.o.d.}$, where $f^{o.o.d.}$ is an estimator with high prediction performance on both training and test domain, and that $f(x) = f^{o.o.d.}(x)$ for sample x from training domains. Under the setting, they deduce a upper bound of a risk on a test domain, and then, propose a method for decreasing the upper bound.

H Additional Experiment

H.1 Additional Experiments of Colored MNIST in Section 6

Although the Colored MNIST experiment in Section 6 fixes its flip rate to 25%, we additionally demonstrate by changing its flip rate among $\{10\%, 15\%, 20\%, 25\%\}$.

Table 4: Test Acc. of Hierarchical Colored MNIST (5runs)

flip rate	Test Acc. on	Best possible	Oracle	ERM	FT	FF	DSAN	Ours + CV1	Ours + CV2	Ours+TDV
0.25	$e = 0.1$	.750	.715(.001)	.693(.001)	.676(.003)	.677(.002)	.593(.007)	.706(.005)	.664 (.013)	.690 (.008)
	$e = 0.9$			.433 (.004)	.250 (.020)	$.248(.015)$	.073(.003)	.753(.011)	**.618 (.018)**	.657(.008)
0.20	$e = 0.1$	.800	.769(.001)	.800(.001)	.727(.002)	.725(.004)	.639(.003)	.752(.006)	.721 (.015)	.745 (.007)
	$e = 0.9$			.525 (.004)	.368 (.029)	$.364(.011)$	.080(.004)	.576(.014)	**.685 (.019)**	.719 (.004)
0.15	$e = 0.1$	.850	.822(.000)	.802(.002)	.782(.006)	.786(.003)	.682(.002)	.806(.006)	.794 (.008)	.794 (.008)
	$e = 0.9$			.630 (.006)	.493 (.038)	$.512(.019)$	.091(.005)	.673(.006)	**.774 (.006)**	.774 (.006)
0.10	$e = 0.1$	.900	.872(.001)	.848(.002)	.827(.004)	.829(.003)	.593(.007)	.857(.005)	.842 (.008)	.834 (.001)
	$e = 0.9$			.719 (.004)	.611(.016)	$.623(.021)$	.073(.003)	.756(.007)	**.800 (.007)**	.821 (.006)

Table 5: Baselines of CV methods

	Tr-CV	LOD-CV
0.25	.702 (.002)	.590 (.004)
	.597 (.006)	.460 (.197)
0.20	.754 (.004)	.716 (.018)
	.678 (.008)	.692 (.010)
0.15	.801 (.016)	.787 (.004)
	.678 (.008)	.774 (.006)
0.10	.854 (.005)	.836 (.004)
	.751 (.013)	.819 (.008)

Table 6: Means and SEs of $\{$(Accuracy of TDV on $e = 0.9$) -(Accuracy of Each CV on $e = 0.9$) $\}$ (5runs).

	CV I	CV II	Tr-CV	LOD-CV
0.25	.051 (.053)	.040 (.017)	.163 (.006)	.197 (.205)
0.20	.143 (.012)	.034 (.017)	.132 (.008)	.023 (.018)
0.15	.102 (.006)	.000 (.000)	.102 (.007)	.003 (.002)
0.10	.065 (005)	.021 (.010)	.075 (.010)	.005 (.002)

Table 4 and 5 show that, among several CV methods, our method II keeps a high predictive performance regardless of flipping rates. Table 6 the difference between accuracies by TDV and each CV for the same data set with $e = 0.9$. The result verifies that CVII selects preferable hyperparameters with smaller errors.

H.2 Additional Experiments: Colored MNIST II

We conduct an additional Colored MNIST experiment, changing annotation and coloring rules from ones in Section 6. Setting $\mathcal{Y} = [3]$ and $\mathcal{Z} := [2]$, we aim to predict Y^e from digit image data X^e, which is in the three categories $0 - 2$ ($Y^e = 0$), 3 or 4 ($Y^e = 1$) and $5 - 9$ ($Y^e = 2$). The label is changed randomly to one of the rest with a some probability ranging from $\{10\%, 15\%, 20\%, 25\%\}$. The domain index $e \in [0.0, 1.0]$ controls the color of the digit; for $Y^e = 0, 1$, the digit is colored in red with probability e and for $Y^e = 2$ colored in green with probability e. In the experiment, $\mathcal{D}^{e^*} \sim P_{X^{0.1}, Y^{0.1}}$ is drawn with sample size $n^{e^*} = 5000$, and Y^e is predicted based on X^e for $e = 0.1$ and 0.9. Regarding Z^e, we consider the task where we predict $Z^e = 0$ for X^e in $0 - 2$ and $Z^e = 1$ for $3 - 9$ (that is, $g(0) = 0$ and $g(1) = g(2) = 1$). We obtain the final label by flipping with some probability. As the domain-specific factor, we color the digit red for $Z^e = 0$ with probability e and green for $Z^e = 1$ with probability e. We set $\mathcal{E}_{ad} = \{0.1, 0.3, 0.5, 0.7, 0.9\}$ with $n^e = 5000$ for $\forall e \in \mathcal{E}_{ad}$. We model Φ by a 3-layer neural net. With the maximum epoch 500, we select (t, λ_{after}) from 3×10 candidates with $t \in \{0, 100, 200\}, \lambda_{after} \in \{10^0, 10^1, ..., 10^9\}$ by each CV method.

Table 7 and 8 shows test accuracies for 2000 random samples in the domains $e = 0.1$ and $e = 0.9$. The results demonstrate that the proposed methods significantly outperform the others for $e = 0.9$. Among the

Table 7: Test Accuracy for Hierarchical Colored MNIST (5runs)

flip rate	Test Acc. on	Best passible	Oracle	ERM	FT	FF	DSAN	Ours + CVI	Ours + CVII	Ours+ TDV
0.25	$e = 0.1$	.750	.729 (.004)	.771 (.001)	.771 (.001)	..771 (.001)	.767 (.004)	.727 (.004)	.714 (.013)	.673 (.006)
	$e = 0.9$			.125 (.003)	.128 (.002)	$.131(.002)$	.085 (.003)	.622 (.015)	**.644 (.019)**	.690 (.009)
0.20	$e = 0.1$	.800	.780 (.002)	.796 (.000)	.800 (.001)	.796 (.001)	.789 (.004)	.773 (.003)	.745 (.008)	.738 (.018)
	$e = 0.9$			.177 (.006)	.201 (.004)	$.200(.007)$	.091 (.005)	.644 (.011)	**.707 (.012)**	.732 (.008)
0.15	$e = 0.1$	.850	.828 (.004)	.822 (.000)	.823 (.001)	.824 (.002)	.815 (.002)	.814 (.007)	.797 (.011)	.822 (.001)
	$e = 0.9$			.277 (.007)	.323 (.006)	$.312(.012)$	.091 (.002)	.724 (.037)	**.743 (.020)**	.782 (.012)
0.10	$e = 0.1$	.900	.880 (.004)	.852 (.002)	.855(.001)	.856 (.001)	.833(.003)	.848 (.005)	.848 (.005)	.857 (.005)
	$e = 0.9$			.468 (.002)	.497 (.005)	$.500(.007)$	.106 (.010)	**.792 (.005)**	**.792 (.005)**	.829 (.005)

Table 8: Baselines of CV methods

	Tr-CV	LOD-CV
0.25	.759 (.008)	.362 (.059)
	.459 (.012)	.372 (.037)
0.20	.794 (.004)	.338 (.048)
	.541 (.007)	.334 (.029)
0.15	.834 (.002)	.348 (.031)
	.634 (.008)	.358 (.024)
0.10	.876 (.003)	.502 (.196)
	.708 (.006)	.497 (.194)

two proposed methods, CV II yields the higher test accuracy. Table 9 shows the difference between accuracies by TDV and each CV for the same data set with $e = 0.9$. The results verify that CVII selects preferable hyperparameters with smaller errors.

H.3 Additional Experiment: Synthesized Data

We compared the proposed method with the other approaches using synthesized data with $\mathcal{X} = \mathbb{R}^2$, $\mathcal{Y} = [3]$ and $\mathcal{Z} := [2]$. We used distributions $N_0 := \mathcal{N}(0, 10^2) \times \mathcal{N}(e, 10^2)$, $N_1 := \mathcal{N}(30, 10^2) \times \mathcal{N}(-4e, 10^2)$ and $N_2 := \mathcal{N}(-30, 10^2) \times \mathcal{N}(-e, 10^2)$, where $\mathcal{N}(a, b)$ denotes a normal distribution with its (mean, variance) $= (a, b)$. Given $x \sim N_i$, the task is to predict N_i among $i = 0, 1, 2$. The aim of IL is to ignore the second component of x, as it works as a domain-specific factor. Given $e^* \in \mathbb{N}_{\geq 0}$ ranging from 0 to 50, each experiment draws $\mathcal{D}^{e^*} \sim P_{X^{e^*}, Y^{e^*}}$ with its sample size $n^{e^*} = 2000$, and then predicts Y^{-e^*} from X^{-e^*}. Setting g by $g(0) = 0$ and $g(1) = g(2) = 1$, we draw $\mathcal{D}^e_{ad} \sim P_{X^e, Z^e}$ from $\mathcal{E}_{ad} = \{-100, -50, 0, 50, 100\}$ with its sample size $n^e = 1000$ ($\forall e \in \mathcal{E}_{ad}$). We model Φ by a 3-layer neural net. Setting the maximum epoch 500, we select (t, λ_{after}) from 3×5 candidates with $t \in \{0, 100, 200\}$ and $\lambda_{after} \in \{10^0, 10^1, ..., 10^4\}$ by each of the CV methods.

Table 10 shows the test accuracy of the estimates for $e = -e^*$ over 2000 random samples $(x, y) \sim P_{X^{-e^*}, Y^{-e^*}}$. When $e^* = 0$ and 5, the domain bias of training (e^*) are similar to the one of test ($-e^*$), and hence, the fine-tuning methods yield high performances, which may use biased correlation. As e^* increases, the difference between the training (e^*) and test ($-e^*$) distributions becomes larger, and the previous methods fail to achieve high accuracy. The proposed methods (Ours) keep higher performance than the others even for large e^*. Among the CV methods, our two methods (CVI, CVII) significantly outperform the others for larger e^*. For this data set, CVI and CVII show almost the same performance.

H.4 Additional Experiment: Bird recognition

Our method is applied to the Bird recognition problem [28], which aims to predict three labels Y^e of images X^e: *waterbird* (Y^e= 0), *landbird* (Y^e= 1) and *no bird* (Y^e= 2). The dataset is made by combining background images from the Places dataset [39] and bird images from the CUB dataset [38] in two different ways $\mathcal{E} := \{e_1, e_2\}$. In domain e_1, we prepare three types of image: landbird image with land background, waterbird image with water background, and no bird with land background (Figure 3, left). In domain e_2, we have landbird images with water background, waterbird images with land background, and no bird with water background (Figure 3, right). For the sample of the target task, we used the domain $e^* = e_1$ and generated $n^{e^*} = 8649$ data $\mathcal{D}^{e^*} \sim P_{X^{e_1}, Y^{e_1}}$. The sample in the higher level $\mathcal{D}^e_{ad}$ of (X^e, Z^e), whose label is

Table 9: Means and SEs of $\{$(Accuracy of TDV on $e = 0.9$) -(Accuracy of Each CV on $e = 0.9$) $\}$ (5runs).

	CV I	CV II	Tr-CV	LOD-CV
0.25	.068 (.007)	.046 (.023)	.231 (.013)	.319 (.033)
0.20	.088 (.004)	.025 (.006)	.191 (.014)	.398 (.025)
0.15	.059 (.038)	.039 (.022)	.148 (.019)	.430 (.028)
0.10	.037 (.010)	.037 (.010)	.121 (.008)	.332 (.196)

Table 10: Average Test ACCs and SEs of Synthesized Data on $e = -e^*$ (5 runs): *Oracle* shows the results of the experiments with the first component. The best scores are **bolded**.

	$e^* = 0$	$e^* = 5$	$e^* = 10$	$e^* = 15$	$e^* = 20$	$e^* = 25$	$e^* = 30$	$e^* = 35$	$e^* = 40$	$e^* = 45$	$e^* = 50$
Oracle	906 (.007)										
ERM	.789 (.218)	.791 (.174)	.637 (.188)	.329 (.201)	.324 (.328)	.311 (.260)	.159 (.193)	.140 (.171)	.132 (.161)	.166 (.147)	.051 (.101)
FT	**.899 (.000)**	**.863 (.001)**	.575 (.002)	.568 (.001)	.673 (.103)	.583 (.088)	.402 (.004)	.350 (.001)	.003 (.000)	.000 (.000)	.000 (.000)
FF	**.899 (.000)**	.861 (.002)	.540 (.102)	.568 (.001)	.673 (.102)	.628 (.001)	.401 (.001)	.351 (.002)	.066 (.132)	.000 (.000)	.000 (.000)
DSAN	.684 (.008)	.367 (.016)	.195 (.015)	.112 (.008)	.045 (.008)	.013 (.003)	.006 (.001)	.001(.001)	.000 (.000)	000 (.000)	.000 (.000)
Ours + Our CV I	.799 (.232)	.784 (.231)	**.884 (.021)**	**.875 (.044)**	**.815 (.098)**	**.738 (.209)**	**.865 (.047)**	**.659 (.233)**	**.666 (.285)**	**.776 (.080)**	**.699 (.255)**
Ours + Our CV II	.799 (.232)	.783 (.231)	**.884 (.021)**	**.875 (.044)**	**.815 (.098)**	**.738 (.209)**	**.865 (.047)**	**.659 (.233)**	.563 (.291)	**.776 (.080)**	**.699 (.255)**
Ours + Tr-CV	.790 (.230)	.776 (.225)	.609 (.163)	.491 (.095)	.366 (.147)	.248 (.192)	.376 (.033)	.215 (.168)	.148 (.127)	.189 (.108)	.031 (.138)
Ours + LOD-CV	.662 (.180)	.521 (.145)	.569 (.204)	.538 (.168)	.450 (.158)	.371 (.213)	.641 (.221)	.571 (.221)	.380 (.196)	.423 (.218)	.316 (.127)
Ours + TDV	.915 (.005)	.905 (.006)	.896 (.002)	.895 (.010)	.848 (.059)	.849 (.069)	.887 (.030)	.764 (.152)	.796 (.174)	.848 (.055)	.775 (.179)

landbird ($Z^e = 0$) and *no landbird* ($Z^e = 1$) (*i.e.*, $g(1) = 0$ and $g(0) = g(2) = 1$), is drawn from both e_1 and e_2 with $n^{e_1} = n^{e_2} = 8649$. Here, we use $\mathcal{D}^{e^*}$ as $\mathcal{D}^{e_1}_{ad}$ with labels of $\mathcal{D}^{e^*}$ re-annotated by g. We made a predictor of Y^e based on X^e, and evaluated the test accuracy in the two domains $e = e_1, e_2$. We model Φ by ResNet50 [29]. Setting the maximum epoch 5, we select (t, λ_{after}) from 5×5 candidates with $t \in [5], \lambda_{after} \in \{10^0, 10^1, ..., 10^4\}$ by each CV method.

Figure 3: Visualization of Bird recognition problem

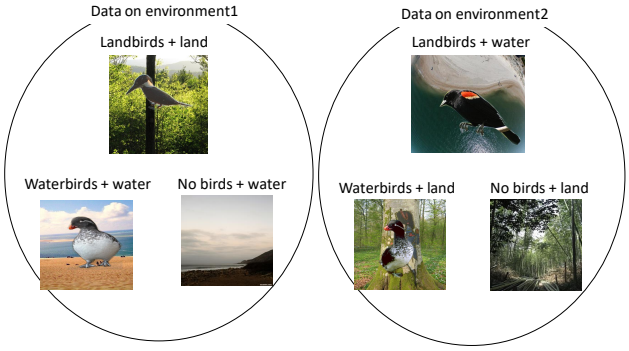

Table 11 shows test accuracies with 2162 random samples for e_1 and e_2. We can see that the proposed framework together with CV methods succeeded in capturing the predictor invariant to the change of background, while the other methods failed. ERM and FT show much higher accuracy for e_1 than Oracle and worst results for e_2, which implies that these methods learn biased correlation in $\mathcal{D}^{e^*}$.

Table 11: Average Test Accuracies and SEs of Bird recognition problem (5 runs). *Oracle* shows a result of ERM with samples from both e_1 and e_2 given. TDV selects λ which yields the highest performance on e_2. Best scores are **bolded**.

	Test Acc. on e_1	Test Acc. on e_2
Oracle	.875 (.018)	
ERM	.902 (.008)	.317 (.044)
FT	.909 (.012)	.364 (.028)
FE	.767 (.024)	.052 (.013)
Ours +Our CV I	.897 (.020)	**.727 (.062)**
Ours +Our CV II	.897 (.020)	**.727 (.062)**
Ours +Tr-CV	.919 (.006)	.651 (.031)
Ours +LOD CV	.338 (.048)	.334 (.029)
Ours +TDV	.886 (.035)	.782 (.020)

H.5 Additional Experiment: ImageNet

In the main body, only test accuracies on e_2 are shown. The result adding test accuracies on the training domain e_1 are as follows:

ImageNet: $\mathcal{Y} = [3], \mathcal{Z} = [2]$.

	Test Acc. on e_1	Test Acc. on e_2
random guess	.333	
Oracle	.743 (.018)	
ERM	.750 (.016)	.417 (.016)
FT	.793 (.018)	.463 (.030)
FF	.439 (.002)	.482 (.117)
DSAN	.288 (.012)	.278 (.004)
Ours + CV I	.843 (.024)	.652 (.028)
Ours + CV II	.852 (.009)	**.666 (.027)**
Ours + Tr-CV	.873 (.009)	.641 (.033)
Ours + LOD CV	.857 (.012)	.525 (.028)
Ours + TDV	.857 (.012)	.673 (.035)

ImageNet: $\mathcal{Y} = [7], \mathcal{Z} = [2]$.

	Test Acc. on e_1	Test Acc. on e_2
random guess	.143	
Oracle	.749 (.008)	
ERM	.740 (.017)	.507 (.020)
FT	.626 (.028)	.409 (.020)
FF	.191 (.004)	.226 (.046)
DSAN	.184 (.012)	.293 (.008)
Ours + CV I	.853 (.006)	**.622 (.011)**
Ours + CV II	.853 (.006)	**.622 (.011)**
Ours + Tr-CV	.850 (.004)	.612 (.012)
Ours + LOD CV	.825 (.017)	.572 (.022)
Ours + TDV	.837 (.019)	.634 (.003)

ImageNet: $\mathcal{Y} = [3], \mathcal{Z} = [2]$.

	Test Acc. on e_1	Test Acc. on e_2
random guess	.333	
Oracle	.743 (.018)	
ERM	.750 (.016)	.417 (.016)
FT	.793 (.018)	.463 (.030)
FF	.439 (.002)	.482 (.117)
DSAN	.288 (.012)	.278 (.004)
Ours + CV I	.843 (.024)	.652 (.028)
Ours + CV II	.852 (.009)	**.666 (.027)**
Ours + Tr-CV	.873 (.009)	.641 (.033)
Ours + LOD CV	.857 (.012)	.525 (.028)
Ours + TDV	.857 (.012)	.673 (.035)

I Experimental Details

I.1 Visualizations of Experiment Results

Synthesized data in Appendix H.3 is visualized as in Figure 4. Synthesized data in the CVs comparison experiment (Section 6) is visualized as in Figure 5.

Figure 4: Synthesized Data in Appendix H.3. Left and middle figures illustrate training and test data on $e^* = 5$ and 50, respectively. As e^* increases, the test data and train data are more different, and therefore ERM yields lower performance. Right figure illustrates $\mathcal{D}_{ad}^{e}$.

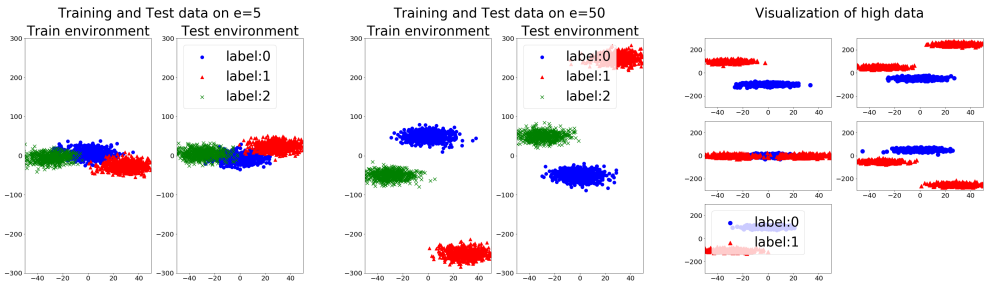

Figure 5: Synthesized Data in Section 6. Left figure illustrates the training and test data of second experiment. Right figure illustrates $\mathcal{D}_{ad}^{40}$ and $\mathcal{D}_{ad}^{e_{ad}}$ with $e_{ad} = -9$.

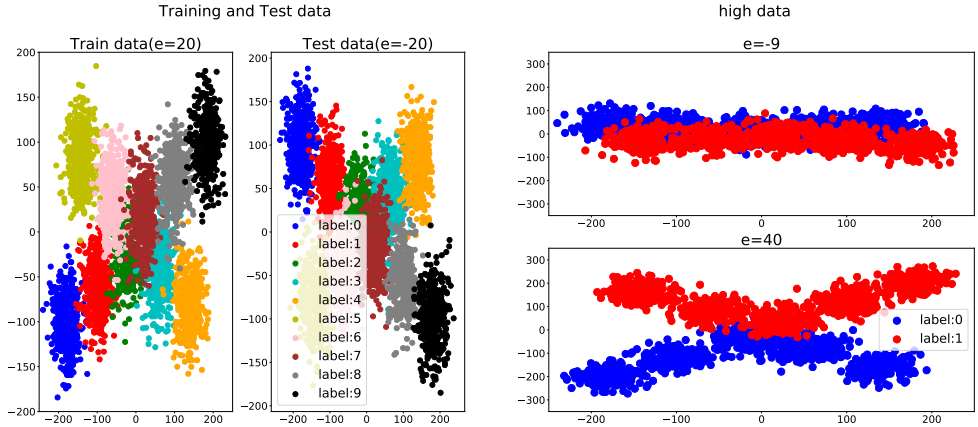

I.2 Explicit representation of Synthetic data used in CV comparison experiment

$$
\begin{aligned}
N_1 &= \mathcal{N}(-180, 20^2) \times \mathcal{N}(-5e, 30^2),\\
N_2 &= \mathcal{N}(-100, 20^2) \times \mathcal{N}(-3e, 30^2),\\
N_3 &= \mathcal{N}(-20, 20^2) \times \mathcal{N}(-1e, 30^2),\\
N_4 &= \mathcal{N}(60, 20^2) \times \mathcal{N}(-2e, 30^2),\\
N_5 &= \mathcal{N}(140, 20^2) \times \mathcal{N}(-4e, 30^2),\\
N_6 &= \mathcal{N}(-140, 20^2) \times \mathcal{N}(4e, 30^2),\\
N_7 &= \mathcal{N}(-60, 20^2) \times \mathcal{N}(2e, 30^2),\\
N_8 &= \mathcal{N}(20, 20^2) \times \mathcal{N}(1e, 30^2),
\end{aligned}
$$

$$N_9 = \mathcal{N}(100, 20^2) \times \mathcal{N}(3e, 30^2),$$
$$N_{10} = \mathcal{N}(180, 20^2) \times \mathcal{N}(5e, 30^2).$$

I.3 Detail of ImageNet experiment data set

In the ImageNet experiment in Section 6, $\mathcal{Y}$ is set as follows:

- $\mathcal{Y} = [3]$:{**bird**, **turtle** ,snake }
- $\mathcal{Y} = [7]$: {**bird**, **turtle**, snake, cat, food, **vehicle**, **building** },
- $\mathcal{Y} = [17]$: {**bird**, **turtle**, snake, cat, **dog**, monkey, spider, butterfly, **food**, **vehicle**, **building**, **shoes**, hat, instrument, tellephone, **bottle**, chair}.

Images of **bolded** labels are composed of different species among e_1 and e_2. Explicitly, dataset are composed as follows:

$$\mathcal{Y} = [3]$$

label	e_1	e_2
bird	ruffed grouse, indigo bunting	albatross, water ouzel
turtle	loggerhead, leathback	.box turtle, mud turtle
snake	thunder snake, garther snake, ringneck. snake	

$$\mathcal{Y} = [7]$$

label	e_1	e_2
bird	ruffed grouse, indigo bunting	albatross, water ouzel
turtle	loggerhead, leathback	.box turtle, mud turtle
snake	thunder snake, garther snake, ringneck. snake	
cat	persian cat, siamese cat, egyptian cat	
food	cucumber, strawberry, pizza	
vechicle	submarine, container ship	golfcart, jeep
building	lighthouse, fountaink	castle, water tower

$\mathcal{Y} = [17]$

label	e_1	e_2
bird	ruffed grouse, indigo bunting	albatross, water ouzel
turtle	loggerhead, leathback	.box turtle, mud turtle
snake	thunder snake, garther snake, ringneck. snake	
cat	persian cat, siamese cat, egyptian cat	
dog	eskimo dog, dalmatian	newfoundland, German shepherd
monkey	guenon, colobus, titi	
spider	wolf spider, garden spider, barn spider	
butterfly	ringlet, monarch, cabbage butterfly	
food	pizza, strawberry	cucumber, broccoli
vechicle	submarine, container ship	golfcart, jeep
building	lighthouse, fountaink	castle, water tower
shoes	clog, sandal	running shoe, loafer
hat	pickelhaube, crash helmet, hat with a wide brim	
instrument	acoustic guitar, electric guitar, violin	
tellephone	cellular telephone, dial telephone, pay-phone	
bottle	pill bottle, pop bottle	beer bottle, wine bottle
chair	barber chair, folding chair, rocking chair	

I.4 model architectures and optimization procedures

Through the experiment in the present paper, all models of competitors are composed of neural networks where its loss function, activation function, and optimizer are cross entropy, Relu Networks and Adam [37]. In the following explanation, NN with its model architecture $a \to h_1 \to \cdots h_k \to h_n \to \mathcal{P}_{[m]}$ means that its input and hidden dimensions are a and $(h_1, ..., h_n)$ respectively, and its output is probability density functions on $[m]$. NN with its model architecture $a \to h_1 \to \cdots h_k \to h_n \to b$ means that its input, hidden and output dimensions are a, $(h_1, ..., h_n)$ and b respectively. All the experiment, we add L^2-reguralized term to our objective function.

We add explanations of previous CV methods. Tr-CV implements cross-validation with using only $\mathcal{D}^*$. In LOD-CV, a model is learnt with excluding one of the $\mathcal{D}^e \subset \mathcal{D}_{ad}$ from $\mathcal{D}_{ad}$, and evaluate its performance by $\mathcal{D}^e$. Changing the role of $e \in \mathcal{E}_{ad}$, and taking their mean, we evaluate final CV-value.

I.4.1 Colored MNIST

We set model architecture of Φ used in our method $2 \to 440 \to 440 \to 440$. We set model architecture of and ERM $2 \to 440 \to 440 \to \mathcal{P}_{[3]}$. When we use FT and FF, its model architecture on pre-train phase and retraining phase are $2 \to 440 \to 440 \to \mathcal{P}_{[2]}$ and $2 \to 440 \to 440 \to \mathcal{P}_{[3]}$ respectively. We set running rate and hyperparameter of L^2-regularized term 0.0004 and 0.002 respectively. When we use $DSAN$, we inherit learning condition in the *Amazon Review dataset* experiment. When training, we use batch learning. We set $K = 10$ of our CV method.

I.4.2 ImageNet

We set model architecture of Φ used in our method ResNet50 [29] with changing its output dimension 256. We set model architecture of and ERM ResNet50 [29] with changing its output $\mathcal{P}_{[3]}$. When we use FT and FF, its model architecture on pre-train phase and retraining phase are ResNet50 [29] with changing its output dimension 2 and 3 respectively. We set running rate and hyperparameter of L^2-regularized term 0.00004 and 0.001 respectively. When training, we use minibatch learning with a minibatch size 56. We set $K = 5$ of each CV method.

I.4.3 CV comparison experiment

We set model architecture of Φ used in our method $2 \to 8 \to 8 \to 1$. We set running rate and hyperparameters of L^2-regularized term 0.05 and 0.001 respectively. When training, we use minibatch learning with dividing $\mathcal{D}^*$, $\mathcal{D}^{e^{ad}}$ and $\mathcal{D}^{40}$ into 50 equal parts respectively. We set $K = 10$ of each CV method.

I.4.4 Appendix: Colored MNIST II

We set model architecture of Φ used in our method $2 \to 440 \to 440 \to 440$. We set model architecture of ERM $2 \to 440 \to 440 \to \mathcal{P}_{[3]}$. When we use FT and FF, its model architecture on pre-train phase and retraining phase are $2 \to 440 \to 440 \to \mathcal{P}_{[2]}$ and $2 \to 440 \to 440 \to \mathcal{P}_{[3]}$ respectively. We set running rate and hyperparameter of L^2-regularized term 0.0004 and 0.002 respectively. When we use $DSAN$, we inherit learning condition in the *Amazon Review dataset* experiment. When training, we use batch learning. We set $K = 10$ of our CV method.

I.4.5 Appendix: Synthesized Data

We set model architecture of Φ used in our method $2 \to 20 \to 20 \to 1$. We set model architecture of ERM $2 \to 20 \to 20 \to \mathcal{P}_{[3]}$. When we use FT and FF, its model architecture on pre-train phase and retraining phase are $2 \to 20 \to 20 \to \mathcal{P}_{[2]}$ and $2 \to 20 \to 20 \to \mathcal{P}_{[3]}$ respectively. We set running rate and hyperparameters of L^2-regularized term 0.0115 and 0.01 respectively. When we use $DSAN$ [31], we inherit learning condition in the *Amazon Review dataset* experiment. When training, we use batch learning. We set $K = 10$ of each CV method.

I.4.6 Appendix: Birds recognition

We set model architecture of Φ used in our method ResNet50 [29] with changing its output dimension 256. We set model architecture of ERM ResNet50 [29] with changing its output $\mathcal{P}_{[3]}$. When we use FT and FF, its model architecture on pre-train phase and retraining phase are ResNet50 [29] with changing its output dimension 2 and 3 respectively. We set running rate and hyperparameter of L^2-regularized term 0.00004 and 0.001 respectively. When training, we use minibatch learning with a minibatch size 56. We set $K = 5$ of each CV method.